J. Fluid Mech. (2008), *vol.* 594, *pp.* 125–156.
doi:10.1017/S0022112007008981 Printed in the United Kingdom

Nonlinear evolution, travelling waves, and secondary instability of sheared-film flows with insoluble surfactants

DAVID HALPERN AND ALEXANDER L. FRENKEL

Department of Mathematics, University of Alabama, Tuscaloosa, AL 35487, USA

(Received 30 March 2007 and in revised form 26 August 2007)

The nonlinear development of the interfacial-surfactant instability is studied for the semi-infinite plane Couette film flow. Disturbances whose spatial period is close to the marginal wavelength of the long-wave instability are considered first. Appropriate weakly nonlinear partial differential equations (PDEs) which couple the disturbances of the film thickness and the surfactant concentration are obtained from the strongly nonlinear lubrication-approximation PDEs. In a rescaled form each of the two systems of PDEs is controlled by a single parameter C, the 'shear-Marangoni number'. From the weakly nonlinear PDEs, a single Stuart–Landau ordinary differential equation (ODE) for an amplitude describing the unstable fundamental mode is derived. By comparing the solutions of the Stuart–Landau equation with numerical simulations of the underlying weakly and strongly nonlinear PDEs, it is verified that the Stuart–Landau equation closely approximates the small-amplitude saturation to travelling waves, and that the error of the approximation converges to zero at the marginal stability curve. In contrast to all previous stability work on flows that combine interfacial shear and surfactant, some *analytical* nonlinear results are obtained. The Hopf bifurcation to travelling waves is supercritical for $C < C_s$ and subcritical for $C > C_s$, where C_s is approximately 0.29. This is confirmed with a numerical continuation and bifurcation technique for ODEs. For the subcritical cases, there are two values of equilibrium amplitude for a range of C near C_s, but the travelling wave with the smaller amplitude is unstable as a periodic orbit of the associated dynamical system (whose independent variable is the spatial coordinate). By using the Bloch ('Floquet') disturbance modes in the linearized PDEs, it transpires that all the small-amplitude travelling-wave equilibria are unstable to sufficiently long-wave disturbances. This theoretical result is confirmed by numerical simulations which invariably show the *large*-amplitude saturation of the disturbances. In view of this secondary instability, the existence of small-amplitude periodic solutions (on the real line) bifurcating from the uniform flow at the marginal values of the shear-Marangoni number does not contradict the earlier conclusions that the interfacial-surfactant instability has a strongly nonlinear character, in the sense that there are no small-amplitude attractors such that the entire evolution towards them is captured by weakly-nonlinear equations. This suggests that, in general, for flowing-film instabilities that have zero wavenumber at criticality, the saturated disturbance amplitudes do not always have to decrease to zero as the control parameter approaches its value at criticality.

1. Introduction

The behaviour of liquid films adjacent to walls is of interest in many industrial and biomedical problems such as coating, material processing, and airway reopening in the lungs (e.g. Halpern *et al.* 2005). Typically, surfactants are present in real films and may play an important role in their behaviour. There has been a considerable amount of work on single-fluid free-surface flows with insoluble surfactants (see, e.g., the recent papers Gao & Lu 2006 and Levy & Shearer 2006). Much less work has been done on flows that have both insoluble surfactants and non-zero interfacial shear of velocity – which is typical, e.g., for two-fluid flows.

Recently, a new instability was uncovered, that of a shear flow of two fluid layers with insoluble surfactant at their interface (see Frenkel & Halpern 2002 and Halpern & Frenkel 2003). The linear behaviour of this long-wave instability has been further investigated in Blyth & Pozrikidis (2004*a*, *b*), Wei (2005*a*, *c*), Frenkel & Halpern (2005) and Wei (2007) (see also Wei & Rumschitzki 2005 and Wei 2005*b* for related work on core-annular flows). The 'interfacial-surfactant' instability is driven by the interaction of the capillary and Marangoni forces with the interfacial shear of the base flow, and does not depend on gravity, inertia or any other factors, for its existence. It disappears if the shear at the interface is zero (Frenkel & Halpern 2002; Halpern & Frenkel 2003), like the classical, surfactantless instability of this flow due to the interfacial jump of viscosity (Yih 1967; see also Hooper 1985 for the semi-infinite geometry case, and Shlang *et al.* 1985 and Hooper & Grimshaw 1985 for weakly nonlinear regimes; for a review, see the book Joseph & Renardy 1993). However, as was mentioned in Frenkel & Halpern (2002), the Yih instability arises as an effect of inertia appearing only in a higher-order correction to the leading-order Stokes approximation, while the interfacial-surfactant instability appears in Stokes' flows. (For the perturbational effects of inertia on the interfacial-surfactant instability, see Frenkel & Halpern 2005.)

In general, for any flows that have both interfacial shear and surfactants, no analytical nonlinear results are known in the literature. Numerically, the nonlinear stages of the 'interfacial-surfactant' instability were studied in Frenkel & Halpern (2006) for the case when one fluid layer is a thin film and the other layer is assumed to be of semi-infinite extent (Blyth & Pozrikidis 2004*a*, *b* included some nonlinear simulations for the complementary case of comparable thicknesses). The evolution of long-wave disturbances of the film thickness and the interfacial surfactant concentration was shown to be governed by a coupled system of strongly nonlinear differential equations (Frenkel & Halpern 2006). Also, a weakly nonlinear limit of the system was documented. It was shown, however, that, in general, the saturation of instability cannot be described by those weakly nonlinear equations because the generic disturbances always grow to become large in the saturated regimes. This fact was uncovered by numerical simulation with periodic boundary conditions on spatial domains which were asymptotically large compared to the marginal wavelength of instability. However, if the periodicity of unstable disturbances is restricted to be close to the marginal wavelength, additional nonlinear terms become essential in the weakly nonlinear partial differential equations (WNPDEs), and the saturation of the instability may possibly occur with small amplitudes. If this really happens, it would mean that there are stationary periodic small-amplitude solutions on the infinite streamwise domain. However, the absence of such small-amplitude solutions in numerical simulations on spatially extended domains indicates that they must be unstable to long-wave disturbances. In the present paper, which includes

analytical nonlinear results, we provide a theory that yields the small-amplitude periodic solutions and also describes their secondary long-wave instability.

The saturation of the infinitesimal disturbances to small-amplitude solutions can be described by a single nonlinear ODE governing a certain amplitude which determines the disturbances of both the film thickness and surfactant concentration. We derive this ODE, the Stuart–Landau equation with a cubic nonlinearity, similar to that pioneered by Stuart (1960) and Watson (1960) (for single-fluid plane parallel flows, in their case). For the long-wave instabilities of film flows with free surfaces, this technique was used in, e.g., Gjevik (1970), Lin (1974), and Cheng & Chang (1990). Similarly, we use a Galerkin type approximation of the disturbances by their fundamental Fourier mode and the first overtone which is nonlinearly excited by the self-interaction of the fundamental. (Actually that overtone consists of two modes due to the two unknown components, the film thickness and the surfactant concentration.) We note that for the two-fluid flows with interfacial shear, but without surfactants, the Stuart–Landau theory was used in Blennerhassett (1980), Renardy (1989) and Chen & Joseph (1991). The Stuart–Landau equation for the case with surfactants, but just single-fluid and without any interfacial shear, was studied recently in Leshansky & Rubinstein (2005).

The rest of the paper is organized as follows. In the next section, starting from the full Navier–Stokes problem (given in appendix A), we use the lubrication and Stokes approximations to obtain a simplified system of coupled equations for the film thickness and the surfactant concentration. The linear stability governed by (the linearization of) these equations is studied in § 3. In § 4, the evolution governed by the Stuart–Landau equation, obtained in appendix B, is compared with the numerical simulations of the underlying weakly and strongly-nonlinear partial differntial equations (SNPDEs). Also, periodic travelling-wave solutions are obtained by using the methods of dynamical systems (for both closed and open flow conditions, similar to, e.g., Scheid *et al.* 2005). The secondary instability of small-amplitude travelling waves is established in § 5. The results are summarized and discussed in § 6.

2. Physical system and governing equations

We consider two immiscible fluid layers in a Couette flow between two shearing parallel plates with an insoluble surfactant on the interface (see figure 1). For simplicity let the densities of the two fluids be equal, which allows one to disregard gravity in the evolution of disturbances. Let y^* be the spanwise, 'vertical', coordinate (the symbol * indicates a dimensional quantity). Let the interface be at $y^* = d_1$, where d_1 is the thickness of the thinner layer, and the y^*-axis is directed from the thinner layer ('film') to the thicker one; we will call this the 'upward' direction (clearly, since there is no gravity, the notions of 'up' and 'down' are a matter of convention). Thus, $d_1 < d_2$ holds, where d_2 is the thickness of the upper fluid. The direction of the 'horizontal' x^*-axis is chosen so that the velocity at the interface is positive, say U_1 (whereas the velocity at the lower plate is zero). We will assume that the aspect ratio is large, $d_2/d_1 >> 1$ (actually, in the zeroth order of the small parameter d_1/d_2, this parameter disappears from the equations, so the upper fluid is effectively semi-infinite, $d_2 = \infty$). For sufficiently slow flow the inertia terms in the Navier–Stokes equations (see Appendix A) are negligible. In the well-known lubrication approximation, which implies that the streamwise characteristic length scale is much larger than the film thickness (see, e.g., the review papers Frenkel & Indireshkumar 1996 and Oron, Davis

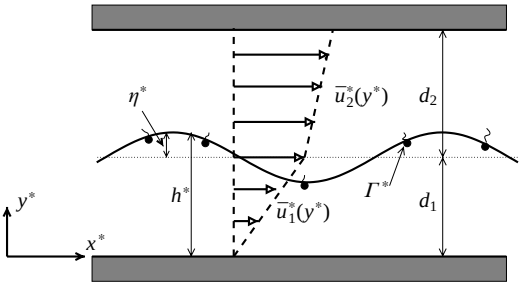

FIGURE 1. Definition sketch for a two-layer plane Couette flow with an interfacial surfactant.

& Bankoff 1997), the simplified dynamic equations for the *disturbances* of velocity components, u and v, and of pressure, p, are, in the dimensionless form,

$$\partial p/\partial x = \partial^2 u/\partial y^2, \tag{2.1}$$

$$\partial p/\partial y = 0, \tag{2.2}$$

$$\partial v/\partial y = -\partial u/\partial x. \tag{2.3}$$

Our dimensionless variables are defined as follows:

$$(x, y) = \frac{(x^*, y^*)}{d_1} \tag{2.4}$$

for the streamwise coordinate x and the crossflow coordinate y;

$$t = \frac{t^*}{d_1\mu_1/\sigma_0} \tag{2.5}$$

for time t, where μ_1 is the film viscosity and σ_0 is the surface tension corresponding to the uniform surfactant concentration $\Gamma^* = \Gamma_0$, whereas in general the surface tension σ^* corresponding to the surfactant concentration Γ^* is assumed to be given by the linear dependence $\sigma^* = \sigma_0 - E\,(\Gamma^* - \Gamma_0)$, where E is a constant; further,

$$(u, v) = \frac{(u^*, v^*)}{\sigma_0/\mu_1} \tag{2.6}$$

for the streamwise velocity component u and the crossflow one v;

$$p = \frac{p^*}{\sigma_0/d_1} \tag{2.7}$$

for the pressure p;

$$\Gamma = \Gamma^*/\Gamma_0 \tag{2.8}$$

for the surfactant concentration Γ; and

$$\sigma = \sigma^*/\sigma_0 \tag{2.9}$$

for the surface tension σ.

In the base (plane Couette) flow, the interface is flat, $\overline{h} = 1$, and the surfactant concentration is uniform, $\overline{\Gamma} = 1$, where the overbar indicates a base-flow quantity. The velocity profiles are linear:

$$\bar{u}_1(y) = ry, \qquad \bar{v}_1 = 0\,, \qquad \text{for } 0 \leqslant y \leqslant 1, \tag{2.10}$$

$$\bar{u}_2(y) = \frac{r}{m}\,(m - 1 + y)\,, \qquad \bar{v}_2 = 0\,, \qquad \text{for } 1 \leqslant y, \tag{2.11}$$

where m is the viscosity ratio, $m = \mu_2/\mu_1$. Clearly, the interfacial shear in the film is given by the parameter r. (Simultaneously, r is the basic velocity of the interface, since the dimensionless film thickness is unity.) It has been shown in Frenkel & Halpern (2006) that the simplified boundary conditions for the disturbances problem (2.1)–(2.3) can be written as follows. The boundary conditions at the lower plate prescribe that

$$u = 0 = v \quad \text{at} \quad y = 0.$$

The terms with disturbance gradients of the semi-infinite layer (in which the lubrication approximation does not hold) are estimated – similarly to, e.g., Babchin *et al.* (1983) – to be negligible in the interfacial boundary conditions (since the characteristic length scales in both directions in the thick layer are large compared to the film thickness, the characteristic y-scale of the film disturbances), at least for m of magnitude-order one. As a result, the simplified normal-stress boundary condition at $y = h(x, t)$ (where h is the film thickness) is written as

$$p = -[1 - M(\Gamma - 1)]h_{xx},$$

and the simplified tangential-stress boundary condition is

$$u_y = -M\Gamma_x,$$

where the Marangoni number M is defined as $M = E\Gamma_0/\sigma_0$. The solution for u in terms of $h(x, t)$ and $\Gamma(x, t)$ is substituted into the mass conservation equation, $h_t + [\int_0^{h(x,t)} u_1(x, y, t)\,\mathrm{d}y]_x = 0$ (where u_1 is the total velocity $u_1 = ry + u$), and the simplified surfactant conservation equation at the interface,

$$\Gamma_t + [\Gamma(rh + u)]_x = 0$$

(in which the small molecular diffusivity of the surfactant has been neglected). As a result, one arrives at the following system of two coupled evolution equations for the film thickness h and the surfactant concentration Γ:

$$h_t + \left(\tfrac{1}{2}rh^2 - \tfrac{1}{2}M\Gamma_x h^2 + \tfrac{1}{3}[(1 + M - M\Gamma)h_{xx}]_x h^3\right)_x = 0, \tag{2.12}$$

$$\Gamma_t + \left[\Gamma\left(rh - M\Gamma_x h + \tfrac{1}{2}h^2[(1 + M - M\Gamma)h_{xx}]_x\right)\right]_x = 0. \tag{2.13}$$

These equations are consistent with earlier studies corresponding to $r = 0$ (e.g., Jensen & Grotberg 1992; Schwartz, Weidner & Eley 1995). (However, $r \neq 0$ is required for the uniform base state to be unstable (Frenkel & Halpern 2002; Halpern & Frenkel 2003)).

We make the simplifying assumptions $M \ll 1$ and $M\Gamma \ll 1$. Rescaling $\tilde{x} = \beta x$ and $\tilde{t} = r\beta t$, where $\beta = (3M/2)^{1/2}$, introducing the constant $C = \beta M/2r = (3M^3/(8r^2))^{1/2}$ (the 'shear-Marangoni number') and dropping the tildes from the new variables, (2.12) and (2.13) take the forms

$$h_t + \left[\tfrac{1}{2}h^2 + C(-\Gamma_x h^2 + h_{xxx}h^3)\right]_x = 0, \tag{2.14}$$

$$\Gamma_t + \left[\Gamma\left(h + C(-2\Gamma_x h + \tfrac{3}{2}h^2 h_{xxx})\right)\right]_x = 0. \tag{2.15}$$

In these simplified equations, a restriction on C comes from the condition that the neglected inertia terms of the Navier–Stokes equations (A 1) be much smaller than the retained viscous terms. Estimating the ratio of these terms, one arrives at the requirement (see, e.g., Frenkel & Indireshkumar 1996) that the modified Reynolds number be small, $\mathrm{Re}\, d_1/L^* \ll 1$, where Re is the Reynolds number based on the interfacial velocity $U_1 = r\sigma_0/\mu_1$ and the thickness d_1, and L^* is the streamwise length

scale of solutions. Using $r = (3/8)^{1/2}M^{3/2}/C$ in the expression for U_1, the validity condition can be written as

$$C \gg M^{3/2}\rho\sigma_0 d_1/(\mu_1^2 L), \tag{2.16}$$

where $L = L^*/d_1$, the dimensionless length scale. (Note that this restriction is still compatible with arbitrarily small values of C – provided, e.g., that M is sufficiently small.)

It is not difficult to obtain weakly nonlinear equations for the disturbances η and g defined by

$$h = 1 + \eta, \quad \Gamma = 1 + g.$$

One assumes the disturbances to be finite but small,

$$\eta \ll 1, \quad g \ll 1,$$

and retains only the leading-order linear and the next-order quadratic terms in η and g in (2.14) and (2.15). Changing to the coordinate $z = x - t$ (which eliminates the term η_x from (2.14) and the term g_x from (2.15)), we obtain the weakly nonlinear system

$$\eta_t + \left(C\eta_{zzz} - Cg_z + \tfrac{1}{2}\eta^2 + 3C\eta\eta_{zzz} - 2C\eta g_z\right)_z = 0, \tag{2.17}$$

$$g_t + \left(\eta + \tfrac{3}{2}C\eta_{zzz} - 2Cg_z + 3C\eta\eta_{zzz} + \eta g - 2C\eta g_z + \tfrac{3}{2}C\eta_{zzz}g - 2Cgg_z\right)_z = 0. \tag{2.18}$$

(If the length scale of the waves is assumed to be large, $\partial/\partial z \ll 1$, then the nonlinear terms inside the parentheses of (2.17) and (2.18) that contain derivatives can be omitted yielding the weakly nonlinear system which we studied in Frenkel & Halpern (2006):

$$\eta_t + \left(\tfrac{1}{2}\eta^2 - Cg_z + C\eta_{zzz}\right)_z = 0, \tag{2.19}$$

$$g_t + \left(\eta g + \eta - 2Cg_z + \tfrac{3}{2}C\eta_{zzz}\right)_z = 0. \tag{2.20}$$

In that case the dominant balance contains just one nonlinear term. However, for the waves whose wavelength is near the marginal value, the dominant balance involves only the linear terms, and in the next order all quadratic terms must be included, as in (2.17) and (2.18)).

For the rest of the paper we will study the system of equations (2.17) and (2.18). Also, for comparison, we include our results of numerical simulation of the original, SNPDE system (2.14) and (2.15).

3. The linear stability properties of the uniform flow

The linear stability theory of this flow has been briefly given in Frenkel & Halpern (2006). Below, we develop the details necessary for the present study.

Neglecting the nonlinear terms in (2.17) and (2.18), we obtain the following linear system for infinitesimal η and g:

$$\eta_t - Cg_{zz} + C\eta_{zzzz} = 0, \tag{3.1}$$

$$g_t + \eta_z - 2Cg_{zz} + \tfrac{3}{2}C\eta_{zzzz} = 0. \tag{3.2}$$

Below we will use a moving reference frame, $\xi = z - V_0 t$. The modified system has additional terms containing the speed V_0 (which remains arbitrary until we make a

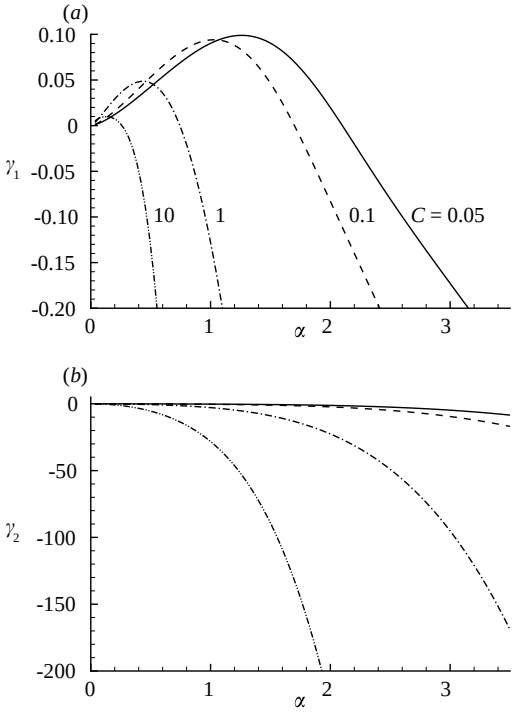

FIGURE 2. Dispersion curves for (*a*) the unstable and (*b*) the stable normal modes for the four values of the parameter C displayed.

specific choice below):

$$\eta_t = V_0\eta_\xi + Cg_{\xi\xi} - C\eta_{\xi\xi\xi\xi}, \tag{3.3}$$

$$g_t = V_0 g_\xi - \eta_\xi + 2Cg_{\xi\xi} - \tfrac{3}{2}C\eta_{\xi\xi\xi\xi}. \tag{3.4}$$

For each wavenumber α there are two different normal modes, of the form ($k = 1, 2$)

$$\begin{bmatrix}\eta\\ g\end{bmatrix} \propto \begin{bmatrix}1\\ g_{k(\alpha)}\end{bmatrix} \mathrm{e}^{\mathrm{i}\alpha\xi}\mathrm{e}^{\gamma_k(\alpha)t}\mathrm{e}^{\mathrm{i}\omega_k(\alpha)t}, \tag{3.5}$$

where the symbol $\propto$ indicates arbitrary scalar multiple, $\gamma_k(\alpha)$ is the growth rate and $\omega_k(\alpha)$ is the frequency. (We note that in terms of α, the validity condition (2.16) is rewritten as $C \gg \alpha M^{3/2}\rho\sigma_0 d_1/\mu_1^2$, since the characteristic length scale is the mode wavelength, $L = 2\pi/\alpha$.) One of the modes, which we assign to $k = 2$, decays for all α, and the other, with $k = 1$, is unstable (provided the shear $r \neq 0$) for 'long' waves, $0 < \alpha < \alpha_0$ (see the dispersion curves in figure 2). Indeed, the amplitude eigenvectors of the two modes,

$$\boldsymbol{v}_1(\alpha) = \begin{bmatrix}1\\ g_{1(\alpha)}\end{bmatrix} \tag{3.6}$$

and

$$\boldsymbol{v}_2(\alpha) = \begin{bmatrix}1\\ g_{2(\alpha)}\end{bmatrix}, \tag{3.7}$$

satisfy the eigenvalue relations (from (3.3) and (3.4))

$$\mathsf{L}_{(\alpha)}\boldsymbol{v}_k(\alpha) = \lambda_{k(\alpha)}\boldsymbol{v}_k(\alpha), \tag{3.8}$$

where

$$\mathsf{L}_{(\alpha)} = \begin{bmatrix} \mathrm{i}V_0\alpha - C\alpha^4 & -C\alpha^2 \\ -\mathrm{i}\alpha - \frac{3}{2}C\alpha^4 & \mathrm{i}V_0\alpha - 2C\alpha^2 \end{bmatrix} \tag{3.9}$$

and

$$\lambda_{k(\alpha)} = \gamma_k(\alpha) + \mathrm{i}\omega_k(\alpha). \tag{3.10}$$

The eigenvectors $v_k(\alpha)$ in (3.8) are determined by

$$g_{k(\alpha)} = -\alpha^2 - \frac{\Lambda_{k(\alpha)}}{C\alpha^2}, \tag{3.11}$$

where

$$\Lambda_{k(\alpha)} = \lambda_{k(\alpha)} - \mathrm{i}\alpha V_0 \tag{3.12}$$

are the two solutions ($k = 1, 2$) of the characteristic quadratic equation

$$\Lambda_{k(\alpha)}^2 + C\alpha^2(2+\alpha^2)\Lambda_{k(\alpha)} + C\alpha^2\left(\tfrac{1}{2}C\alpha^4 - \mathrm{i}\alpha\right) = 0. \tag{3.13}$$

One of the roots here, designated $\Lambda_{2(\alpha)}$, is found to have its real part $\gamma_2(\alpha)$ negative for all α (except $\gamma_2(0) = 0$); the other root is found to have a positive marginal wavenumber α_0 such that $\gamma_1(\alpha) > 0$ for $0 < \alpha < \alpha_0$, with $\gamma_1(\alpha_0) = 0$, and $\gamma_1(\alpha) < 0$ for $\alpha > \alpha_0$.

We choose V_0 to be such that $\omega_1(\alpha_0) = 0$; then, since $\gamma_1(\alpha_0) = 0$, the marginal disturbance is steady in this reference frame: $\lambda_{1(\alpha_0)} = 0$. Hence, (3.12) becomes $\Lambda_{1(\alpha_0)} = -\mathrm{i}\alpha_0 V_0$, and the real part of the quadratic equation (3.13) yields

$$V_0 = -\frac{1}{2+\alpha_0^2}. \tag{3.14}$$

Using this to eliminate V_0 in the imaginary part of quadratic equation (3.13), one finds the marginal wavenumber corresponding to a given C:

$$\alpha_0 = \left(\left(1 + \frac{2^{1/2}}{C}\right)^{1/2} - 1\right)^{1/2}. \tag{3.15}$$

Correspondingly, the marginal C_0 for a fixed α is

$$C_0 = \frac{\sqrt{2}}{\alpha^2(2+\alpha^2)}. \tag{3.16}$$

From (3.14), V_0 depends on C only via α_0.

Figure 2 shows typical dispersion curves representing the dependence of the growth rate on the wavenumber for the two modes with a few representative values of C. They illustrate the long-wave character of the instability. (In the limit of small α, the first and the last (out of the five) terms of the dispersion equation (3.13) are in dominant balance. This gives the long-wave growth-rate asymptotics $\gamma_1(\alpha) \approx \sqrt{C}\alpha^{3/2}$. As a check, when translated back to the original non-dimensionalization units of measurement, the obtained asymptotics coincides with the corresponding result of Frenkel & Halpern 2002 (see also Wei 2007). For $C = 0$, which implies the Marangoni number $M = 0$, the growth rate is zero at any wavenumber – as it should be in the absence of Marangoni forces. As C decreases to 0, the maximum value can grow as is seen in the figure, but with the corresponding wavenumber α_{max} growing to infinity, so that at any fixed α the limit of the growth-rate function is still zero. Then, there is no singularity at $C = 0$: there is convergence, albeit of the non-uniform type, to

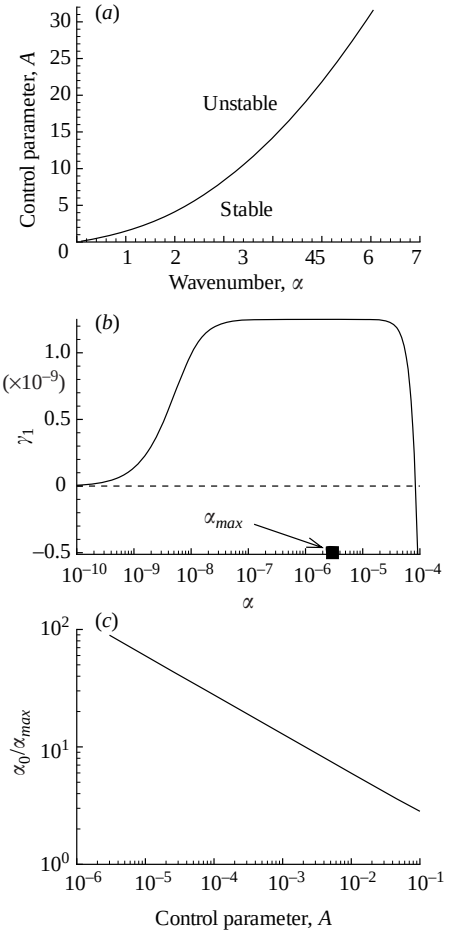

FIGURE 3. (*a*) Marginal stability curve in the plane of wavenumber α and the control parameter $A = C^{-1/2}$ has a criticality point at the zero wavenumber; (*b*) dispersion relation for $A = 10^{-4}$; and (*c*) the ratio of the marginal wavenumber α_0 to the maximum-growth one α_{max} for $A \ll 1$.

the limiting function which is the zero function, $\gamma_1(\alpha) = 0$ for all α. If, in addition to just examining the properties of (2.17)–(2.18) in abstract, one considers their relation to the physical system, it should be noted that the condition (2.16) is equivalent to $r \ll \alpha^{-1}\mu_1^2/(\rho\sigma_0 d_1)$; so, for a given α, the parameter C is not allowed to go to zero in the way of increasing the shear r to infinity. Instead, the limit $C \to 0$ means $M \to 0$. Similarly, the opposite limit, $C \to \infty$, means $r \to 0$, since it has been assumed from the beginning that $M \ll 1$.) Figure 3(*a*) is the curve of marginal stability showing the dependence between the control parameter $A = C^{-1/2}$ and the marginal wavenumber α_0 as determined by (3.15). (In the limit of $A \ll 1$, the asymptotic behaviour is linear, $A \approx \sqrt[4]{2}\alpha_0$. In the opposite limit, $A \to \infty$, one finds $A \approx 2^{-1/4}\alpha_0^2$.) Figure 3(*b*), the dispersion curve for a small value of A (or, correspondingly, very large C), introduces the wavenumber α_{max} of the fastest-growing mode. (Also, note the significant difference of this case, small A, from the cases with $A \gtrsim 1$ of figure 2: in the former case, the band of modes of nearly maximum growth rates extends over many decades. In addition figure 3(*c*) suggests that $\alpha_0/\alpha_{max} \propto A^{-1/3}$, and thus $\alpha_{max} \ll \alpha_0$ at $A \ll 1$, whereas α_0 and α_{max} are of the same magnitude order for $A \gtrsim 1$. These facts

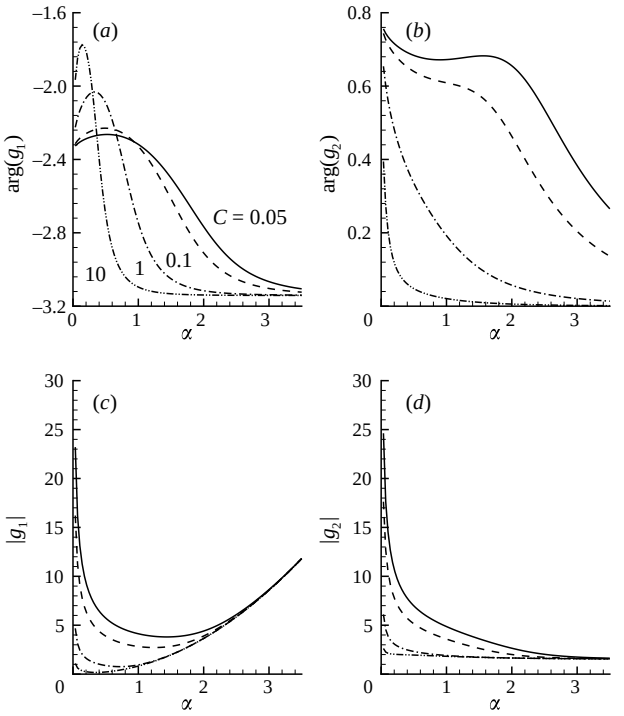

FIGURE 4. Quantities characterizing the basic vectors $\boldsymbol{v}_k$, $k = 1, 2$ (see (3.6) and (3.7)) vs the wavenumber α: arg(g_k), the phase shifts between the thickness deviation and surfactant concentration, in (*a*) and (*b*); $|g_k|$, the amplitude ratios of the thickness deviation and surfactant concentration, in (*c*) and (*d*).

are essential for some of the considerations below). The phase shift between η and g for the two modes, arg($g_{k(\alpha)}$), and the amplitude ratios $g_{max}/\eta_{max} = |g_{k(\alpha)}|$ as functions of α and C are shown in figures 4 and 5. The velocities $V_k = \omega_k/\alpha$ of normal modes are shown in figure 6.

Multiplying (3.3) by η and (3.4) by g, integrating them over the interval of spatial periodicity, and taking into account that η and g are out of phase by nearly π in unstable modes shows that the fourth derivative (capillary) term is stabilizing in (3.3) but destabilizing in (3.4). Similarly, the Marangoni term, the one with $g_{\xi\xi}$, is stabilizing for g but destabilizing with regard to η.

For two-component $2\pi/\alpha$-periodic vector fields on R^1, $[\eta(x), g(x)]^T$, a complete basis consists of $\boldsymbol{u}_1(n)\mathrm{e}^{\mathrm{i}n\alpha x}$ and $\boldsymbol{u}_2(n)\mathrm{e}^{\mathrm{i}n\alpha x}$ where n varies over all integers and, for each n, $\{\boldsymbol{u}_1(n), \boldsymbol{u}_2(n)\}$ is a basis of R^2. In particular, below we choose $\boldsymbol{u}_1(n)$ and $\boldsymbol{u}_2(n)$ to be the eigenvectors $\boldsymbol{v}_k(n\alpha)$ (see (3.6) and (3.7)),

$$\boldsymbol{u}_k(n) = \begin{bmatrix} 1 \\ g_{k(n\alpha)} \end{bmatrix} \tag{3.17}$$

(where $k = 1, 2$). So, any time-dependent vector field $[\eta(x, t), g(x, t)]^T$ such that it is $2\pi/\alpha$ -periodic in space and has the zero spatial mean, can be expanded as

$$\begin{bmatrix} \eta(x,t) \\ g(x,t) \end{bmatrix} = \sum_{n=1}^{\infty} \left(a_n(t) \begin{bmatrix} 1 \\ g_{1(n\alpha)} \end{bmatrix} + b_n(t) \begin{bmatrix} 1 \\ g_{2(n\alpha)} \end{bmatrix} \right) \mathrm{e}^{\mathrm{i}\alpha n x} + \text{c.c.}, \tag{3.18}$$

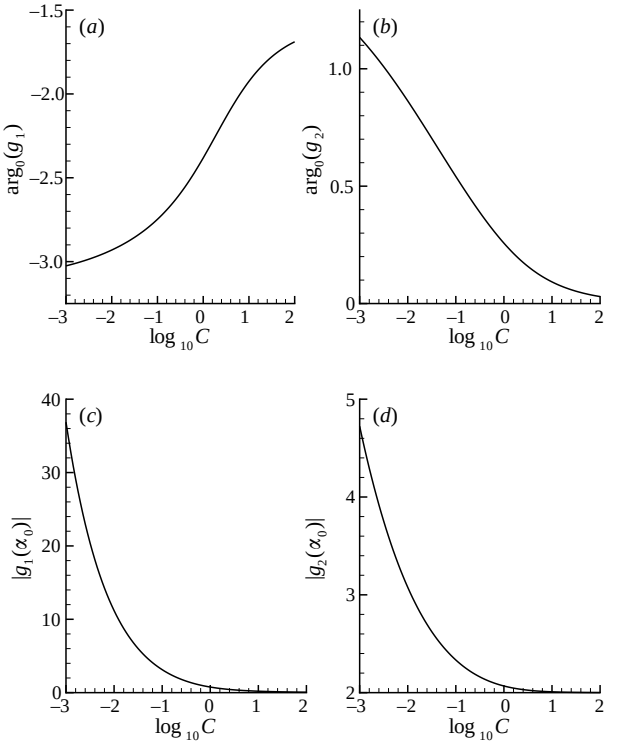

FIGURE 5. The marginal values of the quantities of figure 4 as functions of the parameter C.

where c.c. stands for complex conjugate. (Note that the term with $n = 0$ is absent because of the zero-average condition.)

4. Stuart–Landau evolution

For the wavenumber just below the marginal value (or, if α is fixed, for C just below the value C_0 for which α is the marginal wavenumber), the instability is weak, $\gamma_1 \to 0$ as $\alpha \uparrow \alpha_0$ (or $C \uparrow C_0$). We can expect that the unstable fundamental mode, of wavenumber α, will generate, by the nonlinear interaction with itself, the linearly stable overtones of wavenumber 2α, and the interaction of the latter with the fundamental will lead to the saturation of growth at small amplitudes. (It is also expected that the velocity of saturated travelling waves W is small, $W \to 0$ as $\alpha \uparrow \alpha_0$.) This kind of phenomenon is typically described by the Stuart–Landau equation, which we derive for the present case in appendix B. (We note that due to the translational invariance, in the absence of reflectional symmetry for all the evolution systems of equations here, e.g., (2.17)–(2.18), the problem with periodic boundary conditions has SO(2) symmetry, and the primary bifurcations from the uniform state are the Hopf bifurcations yielding travelling waves (see, e.g., Golubitsky, Stewart & Schaeffer 1988)). We expect the amplitude of the fundamental to be of the order $\epsilon^{1/2}$ with ϵ defined as the relative deviation of the 'shear-Marangoni' number C from its marginal value C_0:

$$\epsilon = \frac{C_0 - C}{C_0}. \tag{4.1}$$

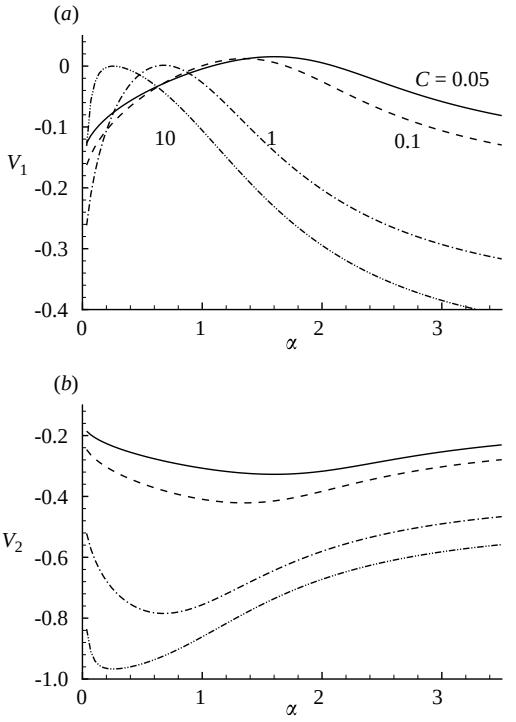

FIGURE 6. Wavenumber dependence of the velocities of (*a*) unstable and (*b*) stable eigenmodes for different values of the parameter C.

The amplitude of the 2α overtone is expected to be of order ϵ and the higher overtones, of wavenumbers $n\alpha$ ($n > 2$), are of higher orders in ϵ. So we can truncate the expansion (3.18) and look for the weakly nonlinear solutions of the form

$$\begin{bmatrix}\eta\\ g\end{bmatrix} = A_{1(\alpha)}(t)\begin{bmatrix}1\\ g_{1(\alpha)}\end{bmatrix}\mathrm{e}^{\mathrm{i}\alpha\xi} + A_{2(\alpha)}(t)\begin{bmatrix}1\\ g_{2(\alpha)}\end{bmatrix}\mathrm{e}^{\mathrm{i}\alpha\xi} + A_{1(2\alpha)}(t)\begin{bmatrix}1\\ g_{1(2\alpha)}\end{bmatrix}\mathrm{e}^{2\mathrm{i}\alpha\xi} + A_{2(2\alpha)}(t)\begin{bmatrix}1\\ g_{2(2\alpha)}\end{bmatrix}\mathrm{e}^{2\mathrm{i}\alpha\xi} + \text{c.c.} + O(\epsilon^{3/2}) \tag{4.2}$$

(where $A_{2(\alpha)}$ is expected to be $O(\epsilon^{3/2})$ as well, but is displayed for the symmetry of the expression).

In Appendix B, a Stuart–Landau equation for the amplitude $A_{1(\alpha)}$ is obtained, (B 18). It readily follows from this equation that

$$\frac{\mathrm{d}|A_{1(\alpha)}|^2}{\mathrm{d}t} = 2\gamma_1(\alpha)|A_{1(\alpha)}|^2 - \ell_r|A_{1(\alpha)}|^4, \tag{4.3}$$

$$\frac{\mathrm{d}\theta}{\mathrm{d}t} = \omega_1(\alpha) - \frac{1}{2}\ell_i|A_{1(\alpha)}|^2, \tag{4.4}$$

where θ is the phase of $A_{1(\alpha)}$, so that $A_{1(\alpha)} = |A_{1(\alpha)}|\mathrm{e}^{\mathrm{i}\theta}$, and ℓ_r and ℓ_i are the real and imaginary parts of ℓ, respectively ($\ell = \ell_r + \mathrm{i}\ell_i$). If the initial amplitude is small, the nonlinear term is negligible and the disturbance grows exponentially. As a result, the nonlinear term grows faster than the linear one. If $\ell_r > 0$, this leads to a saturated state, a fixed point of the dynamical system, for which the time derivative is zero and

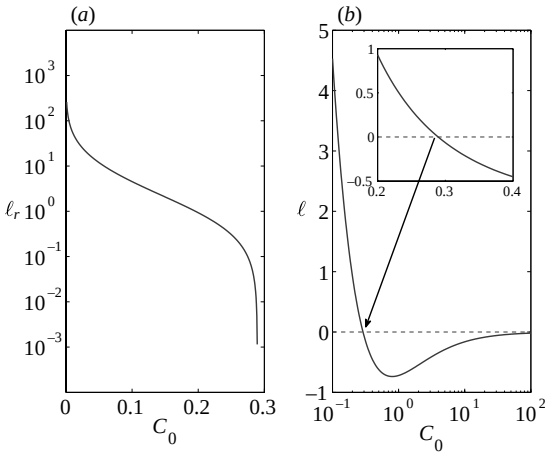

FIGURE 7. The real part of the Landau constant versus the parameter C_0 for (*a*) the range of small C_0 and (*b*) a range of larger C_0. The inset in (*b*) zooms in on the range of C_0 in which ℓ_r changes sign.

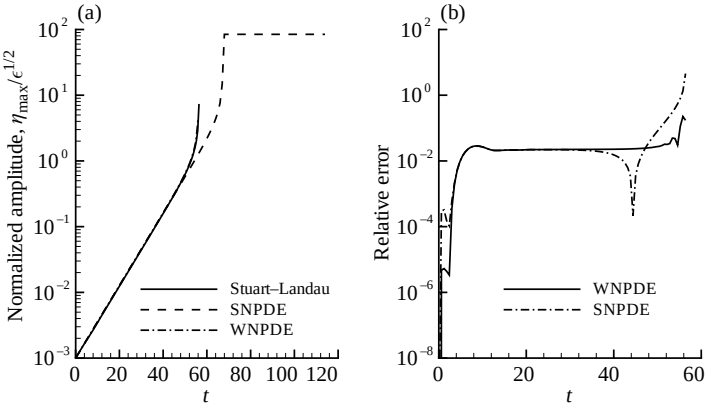

FIGURE 8. (*a*) Evolutions of the quantity $\eta_{max}/\epsilon^{1/2}$ for a case with a negative Landau parameter ℓ_r (here, $C_0 = 0.5$): a large amplitude saturation for the SNPDE (here, with $\epsilon = 10^{-4}$) but a blow-up for both the Stuart–Landau ODE and WNPDE evolutions; (*b*) relative error between the Stuart–Landau equation and the indicated PDEs.

thus

$$|A_{1(\alpha)}|^2 = 2\frac{\gamma_1(\alpha)}{\ell_r}. \tag{4.5}$$

However, as figure 7 testifies, the quantity ℓ_r becomes negative when C is greater than a threshold value $C_s \approx 0.29$. For the negative values of ℓ_r, the instability does not saturate at small amplitudes and the disturbance grows out of the validity range of the Stuart–Landau equation. Such an evolution is shown in figure 8 along with the corresponding solutions of the WNPDEs and the SNPDEs. We discuss details in a separate subsection that follows the next one (the latter tackles the opposite case, that of positive ℓ_r).

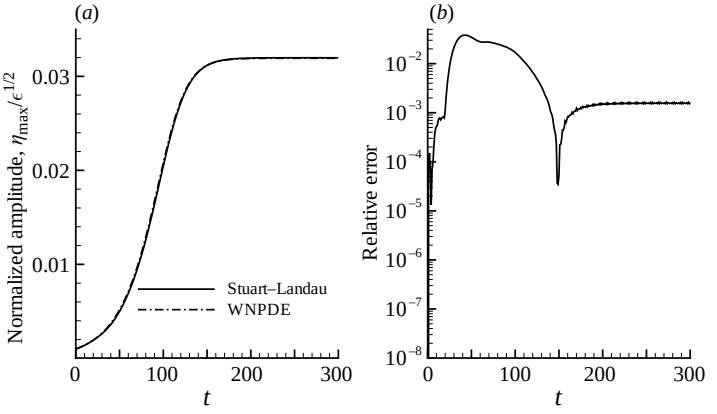

FIGURE 9. (*a*) Evolutions of the quantity $\eta_{max}/\epsilon^{1/2}$ for a case with a positive ℓ_r: small-amplitude saturation (here $C_0 = 10^{-3}$ and $\epsilon = 10^{-4}$); (*b*) relative error between the Stuart–Landau equation and the WNPDE.

4.1. *Stuart–Landau travelling waves*

With positive ℓ_r, (4.4) and (4.5) yield a linear dependence of θ on time, $\theta = \Omega t$ at large t, where

$$\Omega = \left(\omega_1(\alpha) - \gamma_1(\alpha)\frac{\ell_i}{\ell_r}\right). \tag{4.6}$$

The saturated solution describes a travelling wave of the length $2\pi/\alpha$. It corresponds to the Hopf bifurcation of the dynamical system to the limit cycle with the period $2\pi/\Omega$. The Hopf bifurcation is supercritical: the amplitude (4.5) goes to zero as $\epsilon \downarrow 0$. It is also degenerate, in the sense that the frequency (4.6) goes to zero as $\epsilon \downarrow 0$. We note that the period $2\pi/\Omega$ depends on the reference frame. It becomes infinite (at a fixed finite ϵ) in the 'comoving' reference frame, given by $\zeta = \xi - Wt$, where W is determined from

$$\omega_1(\alpha) - \gamma_1(\alpha)\frac{\ell_i}{\ell_r} - \alpha W = 0 \tag{4.7}$$

with $\omega_1(\alpha)$ and ℓ_i/ℓ_r depending on W, since $V_0 + W$ takes the place of V_0 in relations such as (3.12). The zero Ω corresponds to a time-independent solution (which is still $2\pi/\alpha$ periodic in space).

In figure 9 we show a typical solution of the Stuart–Landau equation compared with the solution of the full (weakly nonlinear) PDEs (2.17) and (2.18) with the same parameter values and initial conditions. The agreement is very good. We have also checked (not shown here) that for this range of (sufficiently small) C in which the amplitudes remain small for all time, the WNPDEs give a good approximation to the strongly nonlinear evolution for all time.

As figure 10 illustrates, the relative error of the Stuart–Landau equation decreases with ϵ (asymptotically, as $\epsilon^{1/2}$). Figure 11 shows the dependence (in the ζ frame) of the normalized saturated amplitude, $|A_{1(\alpha)}|\epsilon^{-1/2}$, on C. (The quantity $|A_{1(\alpha)}|$ determines the amplitude of η.)

4.2. *The range of subcritical bifurcation*

As figure 8 shows, in this range of (larger) C, the strongly nonlinear evolution still leads to saturation, but at large amplitudes, which are beyond the range of validity

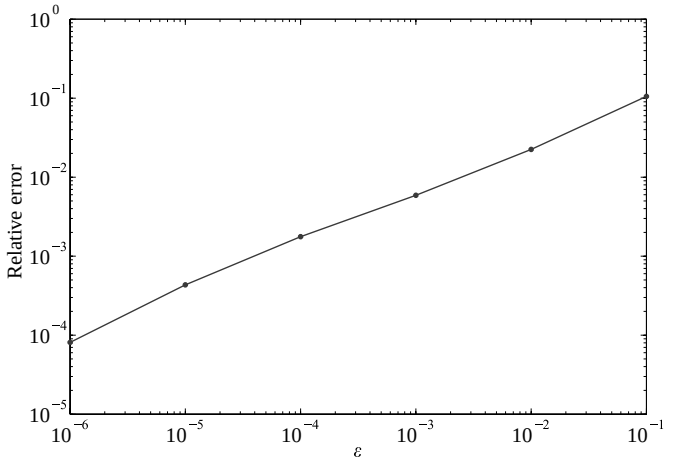

FIGURE 10. The relative error of the Stuart–Landau equation decreases with ϵ.

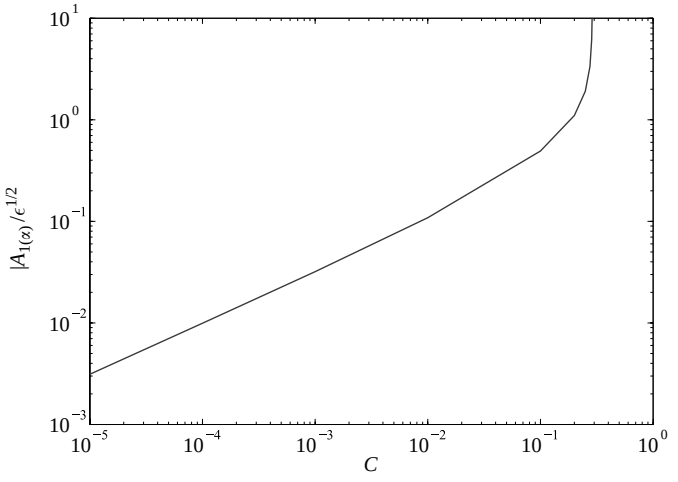

FIGURE 11. Normalized saturated amplitude as a function of C.

of both the Stuart–Landau and the weakly nonlinear equations. All three evolutions are close as long as the amplitudes are still small, but diverge from one another at large amplitudes. The bifurcation from the flat solution at the marginal value of α in this range of C is subcritical in contrast to the supercritical bifurcation at smaller C (discussed in the previous subsection).

4.3. *Dynamical systems approach*

These conclusions about the character of the bifurcation are corroborated by looking for travelling-wave solutions as periodic solutions of a dynamical system in which the spatial coordinate is the independent variable. In the reference frame which moves with the same velocity W_1 as the travelling wave does, the solution does not depend on time, so that the time-derivative term disappears from (2.14) and (2.15), which

thus become just ODEs:

$$\left[-W_1 h + \left(\tfrac{1}{2}h^2 + C(-\Gamma' h^2 + h''' h^3)\right)\right]' = 0, \tag{4.8}$$

$$\left[-W_1 \Gamma + \left(\Gamma\left(h + C\left(-2\Gamma' h + \tfrac{3}{2}h^2 h'''\right)\right)\right)\right]' = 0, \tag{4.9}$$

where $'$ stands for the derivative with respect to the spatial variable $\zeta = x - W_1 t$ (note the relation between the mutual velocities of the different reference frames used here: $W_1 = W + V_0 + 1$). Integrating once, these become

$$-W_1 h + \left(\tfrac{1}{2}h^2 + C(-\Gamma' h^2 + h''' h^3)\right) = Q,$$

$$-W_1 \Gamma + \left(\Gamma\left(h + C(-2\Gamma' h + \tfrac{3}{2}h^2 h''')\right)\right) = \Phi,$$

where Q and Φ are the integration constants. Assuming that $h \neq 0$ and $\Gamma \neq 0$, h''' and Γ' can be expressed in terms of h and Γ:

$$h''' = F[h, \Gamma] = \frac{1}{Ch^2}\left(\frac{4Q}{h} - \frac{2\Phi}{\Gamma} + 2W_1\right), \tag{4.10}$$

$$\Gamma' = G[h, \Gamma] = \frac{1}{Ch}\left(\frac{3Q}{h} - \frac{2\Phi}{\Gamma} + W_1 + \frac{1}{2}h\right) \tag{4.11}$$

(where we have introduced the new functions F and G). The above set of equations can be rearranged as a four-dimensional dynamical system of (autonomous) differential equations:

$$U_1' = LU_2,\ U_2' = LU_3,\ U_3' = LF[U_1, U_4],\ U_4' = LG[U_1, U_4], \tag{4.12}$$

where $U_1 = h$, $U_2 = h'$, $U_3 = h''$, $U_4 = \Gamma$, $L = 2\pi/\alpha$, and the symbol $'$ now indicates differentiation with respect to $\xi = \zeta/L$. The continuation and bifurcation software for ODEs AUTO-07P (Doedel *et al.* 2006) was used to determine periodic solutions of (4.12). To ensure spatial periodicity, the following boundary conditions are applied:

$$U_1(0) = 1, \quad U_i(1) = U_i(0) \quad \text{for} \quad i = 1, 2, 3, 4. \tag{4.13}$$

In addition, the following two integral conservation constraints are imposed:

$$\int_0^1 U_1(\xi)\,\mathrm{d}\xi = 1 \quad \text{and} \int_0^1 U_4(\xi)\,\mathrm{d}\xi = 1. \tag{4.14}$$

These constraints and the first condition of (4.13) are appropriate for the so-called 'closed flow conditions'. (For a detailed discussion of the closed and open flow conditions, see e.g., Scheid *et al.* (2005).)

A certain number of free parameters must exist in order for AUTO to carry out a continuation calculation. For a boundary value problem, that number is $NBC + NINT - NDIM - 1$, where NBC is the number of boundary conditions, $NINT$ is the number integral constraints and $NDIM$ is the order of the system of differential equations. For our problem, the number of free parameters is four: α, Q, Φ, W_1. The starting point for the continuation is the marginal mode with $\alpha = \alpha_0$, $W_1 = V_0 + 1$, $Q = -W_1 + 1/2$ and $\Phi = -W_1 + 1$. In order to obtain non-trivial solutions at the start of the continuation, a small-amplitude perturbation is added to the basic uniform profiles of the dependent variables U_i, namely to $\bar{U}_1 = \bar{U}_4 = 1$ and $\bar{U}_2 = \bar{U}_3 = 0$.

The bifurcation diagrams for different characteristics of the travelling waves are shown in figure 12. (We have followed only the primary bifurcations from the uniform state, because we are interested in *small-amplitude* travelling waves only. Also, similarly to Scheid *et al.* (2005), we do not show the multihump solutions, which are just trains

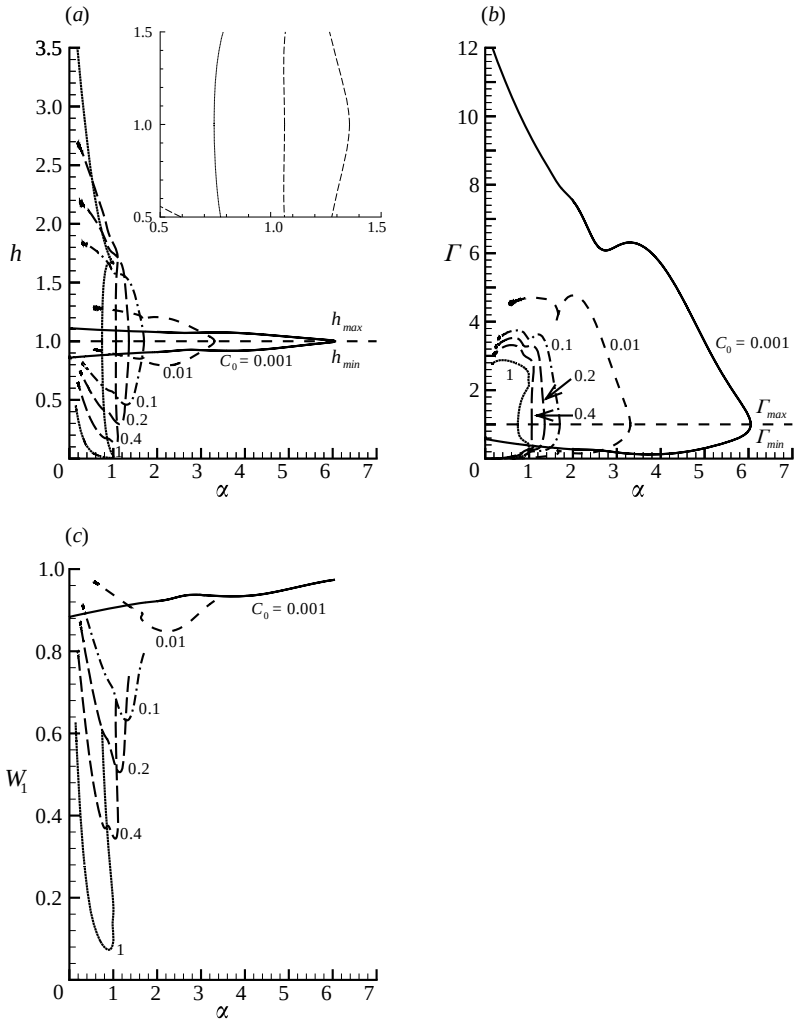

FIGURE 12. Characteristics of the travelling waves as functions of the wavenumber α for several values of C_0 identified next to the curves, for closed flow conditions: (*a*) the maximum and minimum film thickness; (*b*) the maximum and minimum surfactant concentration; and (*c*) the wave speed.

of n identical single-hump profiles, where $n = 2, 3, \ldots$). In particular, one can see in figure 12 that there is a value C_s of C, confined to the interval $0.2 < C_s < 0.4$ (more precisely, as was noted before in the discussion of figure 7, $C_s \approx 0.29$), such that the bifurcation from the basic uniform flow is supercritical for $C < C_s$ but becomes subcritical for $C > C_s$. For the subcritical continuation curves, there is a region of wavenumbers delimited below by the marginal one, for which there are two amplitude values at each wavenumber. As is usual in such cases, only the equilibrium with the larger amplitude is stable (as a periodic orbit of the dynamical system) and the other one is unstable. The profiles of travelling waves are shown in figure 13. As the wavenumber is decreased from its marginal value, the profiles become progressively less sinusoidal, and the amplitudes grow. Also, long stretches of flat film and uniform surfactant concentration appear in the profiles at the smaller values of α. One notices

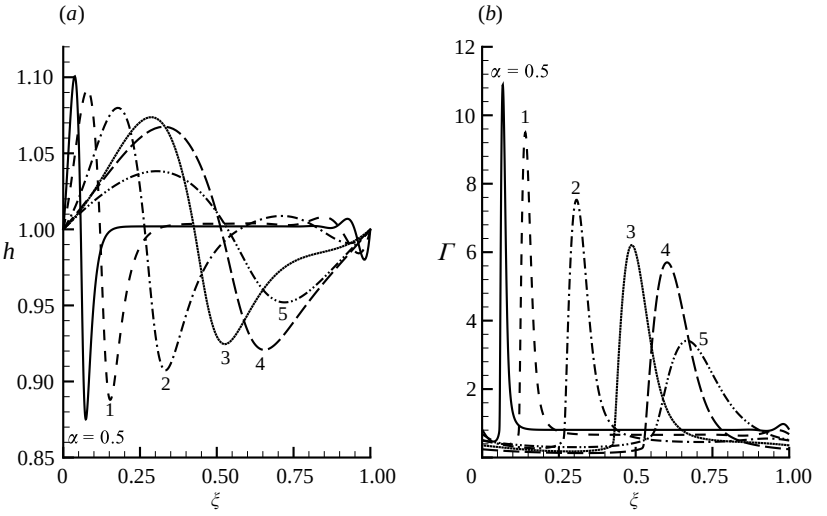

FIGURE 13. Travelling-wave profiles for one spatial period (closed flow conditions) for several values of the wavenumber α ($C = 10^{-3}$): (*a*) film thickness profiles, and (*b*) surfactant concentration profiles.

that some smaller waves in the profile are seen for $\alpha = 2$ and smaller values of α. However, they appear at the back of the film thickness pulse (whose front is indicated by the largest slope) instead of the usual 'bow waves' in front of the pulse. Also, one can see that the pulses of the surfactant concentration are steeper at the back than at the front of the pulse.

The latter property though is not universal. Figure 14, which documents the situation at a larger value of the shear-Marangoni parameter, namely $C = 1$, has steeper fronts of the concentration pulses for some α and steeper backs for other α. Also, the flat parts of the film profile have very small thicknesses, especially for some intermediate values of α. Along with these 'dry spots' in film-thickness profiles, there are 'depleted spots' in the profiles of surfactant concentration, where its value is close to zero. The variation of the film thickness, $h_{max} - h_{min}$, is large in contrast to the cases with small C. On the other hand, the variation of surfactant concentration decreases with C.

4.4. *The open flow condition*

The space-periodic boundary conditions are appropriate for closed flows, such as the one in a closed toroidal channel (e.g. one with a rectangular cross-section and with one of the flat annular walls rotating, as in Barthelet, Charru & Fabre 1995 and Dong & Johnson 2005). For other types of flows, where the fluid flowing out is not reinjected at the inlet, and the disturbance of flux is imposed at the inlet end of the channel, the so-called open flow conditions are pertinent.

While for the closed flow condition, the (spatial) average of the film thickness is conserved during continuation (see, e.g., Scheid *et al.* 2005), for the open flow conditions, the (spatial) average of the volume flux $q = h^2/2 + C(-\Gamma_x h^2 + h_{xxx}h^3)$ is conserved (see (2.14); clearly, $q = W_1 h + Q$ where Q is the flux in the comoving reference frame):

$$\langle q \rangle_\xi = \tfrac{1}{2}, \tag{4.15}$$

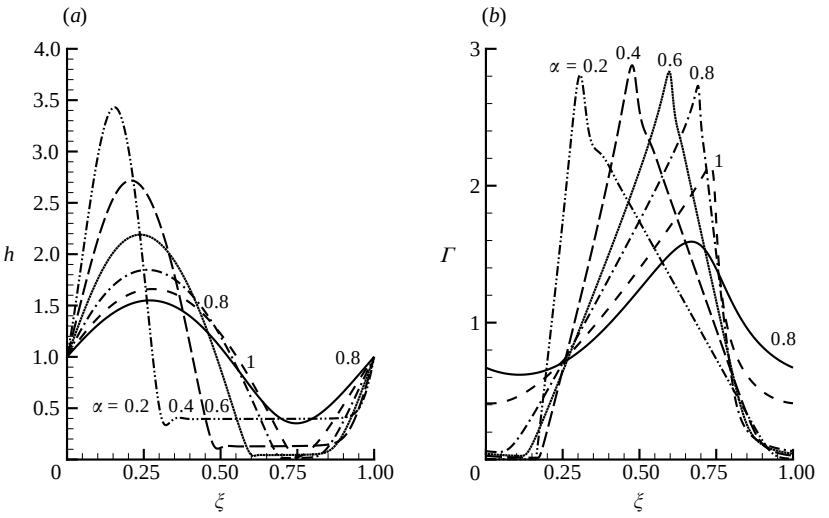

FIGURE 14. Travelling-wave profiles for one spatial period (closed flow conditions) for several values of the wavenumber α ($C = 1$): (*a*) film thickness profiles, and (*b*) surfactant concentration profiles.

where $\langle\cdot\rangle_\zeta = (1/L)\int_0^L \cdot\, \mathrm{d}\zeta = \int_0^1 \cdot\, \mathrm{d}\xi = \langle\cdot\rangle_\xi$. Here, $\frac{1}{2}$ is the flux q of the basic flat-film flow. Similarly, the average flux ϕ of the surfactant concentration is conserved: the relevant equations are $\phi = \Gamma\left(h + C(-2\Gamma_x h + \frac{3}{2}h^2 h_{xxx})\right)$ from (2.15), $\phi = W_1\Gamma + \Phi$ and $\langle\phi\rangle_\xi = 1$. Therefore, for the open flow condition, the integral constraints are as follows:

$$\int_0^1 U_1(\xi)\,\mathrm{d}\xi = \frac{\frac{1}{2} - Q}{W_1} \quad \text{and} \quad \int_0^1 U_4(\xi)\,\mathrm{d}\xi = \frac{1 - \Phi}{W_1}, \tag{4.16}$$

and the boundary condition $U_1(0) = 1$ changes to $U_1(0) =< h >_\xi = (\frac{1}{2} - Q)/W_1$. (It is clear that as long as the resulting profile of h happens to take the value $h = 1$ at some place, the results are identical with those obtained using the condition $U_1(0) = 1$.)

The bifurcation diagrams for the open flow cases appear in figure 15. Figure 15(*b*) shows that the minimum surfactant concentration of the travelling wave becomes larger than 1 at small α, which obviously would be impossible for closed flow cases since for them the *average* value of Γ is 1. The value C_s of C at which the bifurcation becomes subcritical is somewhat larger than the one for the closed flow case: $0.4 < C_s < 0.6$. The spatial profiles of travelling waves for open flow cases appear in figures 16 and 17. They are similar to the closed flow cases when C is small. However, for large C, in contrast to closed flow cases, there are no extended stretches of uniform film thickness and surfactant concentration. Instead, the film thickness tends to zero at just a single point, and the surfactant concentration develops a steep front.

5. The secondary instability

In the comoving reference frame, (see (4.7)), the saturated solution is time-independent and periodic in space (see (4.2)):

$$[\eta, g]_s^T = [N_1, G_1]^T \mathrm{e}^{\mathrm{i}\alpha\zeta} + [N_2, G_2]^T \mathrm{e}^{2\mathrm{i}\alpha\zeta} + \text{c.c.} \tag{5.1}$$

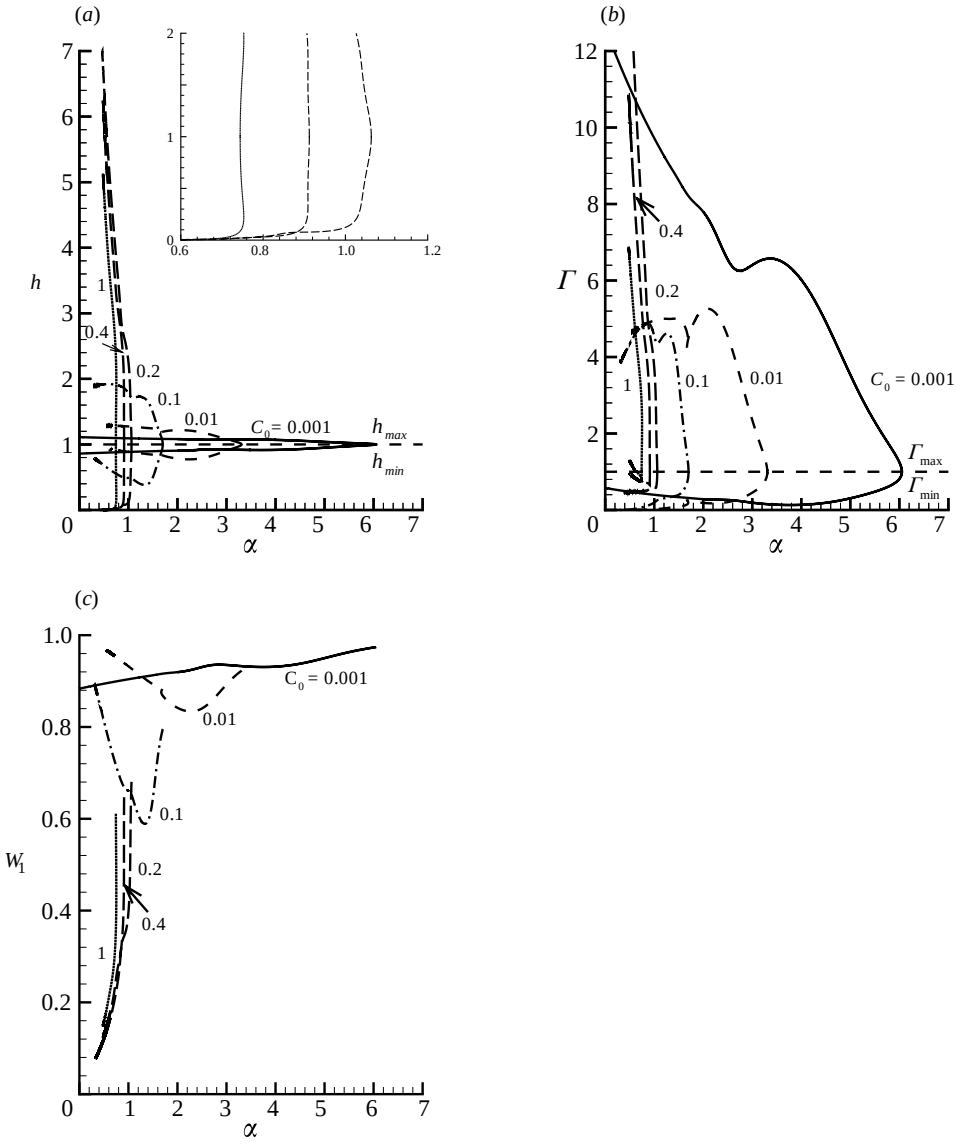

FIGURE 15. Characteristics of the travelling waves as functions of the wavenumber α for several values of C_0, for open flow conditions: (*a*) The maximum and minimum film thickness; (*b*) the maximum and minimum surfactant concentration; and (*c*) the wave speed.

Here N_1, N_2, G_1 and G_2 are defined in terms of the saturated amplitudes as follows: $N_1 = A_{1(\alpha)}$, $N_2 = A_{1(2\alpha)} + A_{2(2\alpha)}$, $G_1 = A_{1(\alpha)}g_{1(\alpha)}$ and $G_2 = A_{1(2\alpha)}g_{1(2\alpha)} + A_{2(2\alpha)}g_{2(2\alpha)}$. (We have kept the terms $O(\epsilon^{1/2})$ and $O(\epsilon)$, and neglected terms $O(\epsilon^{3/2})$, such as those containing $A_{2(\alpha)}$.) These coefficients can, in principle, be found analytically using (3.13), (3.14), (3.12), (3.11), (3.10), (B 8), (B 10), (B 20), (4.5), (4.6) and (B 17), which only involves solving algebraic equations of degree at most four. However, the formulas are not simple, and in practice it is more convenient to solve the quadratic equation (3.13) and the quartic equation (4.7) by standard numerical methods.

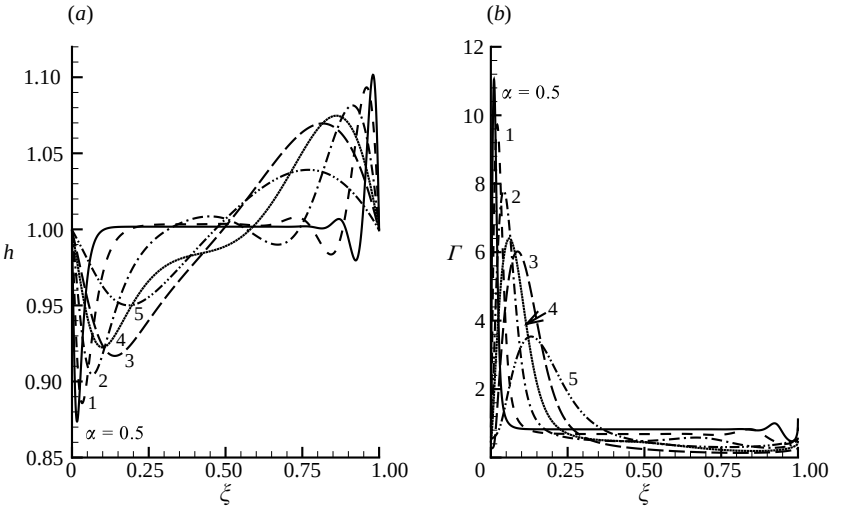

FIGURE 16. Travelling-wave profiles for one spatial period (open flow conditions) for several values of the wavenumber α ($C = 10^{-3}$): (*a*) film thickness profiles, and (*b*) surfactant concentration profiles.

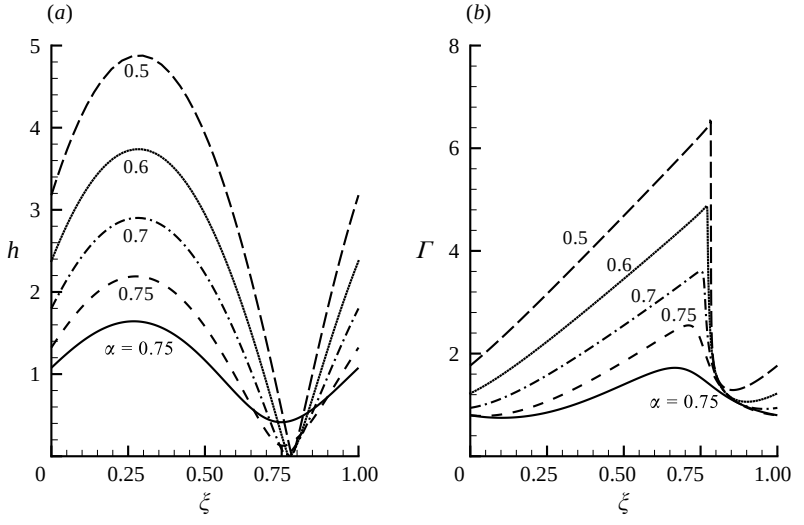

FIGURE 17. Travelling-wave profiles for one spatial period (open flow conditions) for several values of the wavenumber α ($C = 1$): (*a*) film thickness profiles, and (*b*) surfactant concentration profiles.

To study the stability of these time-independent space-periodic states to infinitesimal disturbances, one should consider normal modes of the Bloch type (see, e.g., Kelly 1967, Herbert 1988, Frenkel 1991, Chang, Demekhin & Kopelevich 1993, Indireshkumar & Frenkel 1996; here we closely follow the last paper):

$$[N, G]^T \propto \mathrm{e}^{Pt+\mathrm{i}\alpha K\zeta}\left[\sum_{m=-l}^{l} B_m \mathrm{e}^{\mathrm{i}m\alpha\zeta}, \sum_{m=-l}^{l} C_m \mathrm{e}^{\mathrm{i}m\alpha\zeta}\right]^T. \tag{5.2}$$

We substitute $[\eta, g]^T = [\eta, g]_s^T + [N, G]^T$ into the WNPDEs (see (2.17) and (2.18)) appropriate for the comoving reference frame,

$$\eta_t - (V_0 + W)\eta_\zeta + \left(C\eta_{\zeta\zeta\zeta} - Cg_\zeta + \tfrac{1}{2}\eta^2 + 3C\eta\eta_{\zeta\zeta\zeta} - 2C\eta g_\zeta\right)_\zeta = 0, \tag{5.3}$$

$$g_t - (V_0 + w)g_\zeta + \left(\eta + \tfrac{3}{2}C\eta_{\zeta\zeta\zeta} - 2Cg_\zeta + 3C\eta\eta_{\zeta\zeta\zeta} + \eta g - 2C\eta g_\zeta + \tfrac{3}{2}C\eta_{\zeta\zeta\zeta}g - 2Cgg_\zeta\right)_\zeta = 0, \tag{5.4}$$

and linearize these with respect to N and G. The combined coefficient of $e^{in\zeta}$ in each of (5.3) and (5.4) should vanish for each m ($m = -l, \ldots, 0, \ldots, l$), in view of the linear independence of the exponentials. This yields an eigenvalue problem for the (complex) growth rate P. The eigenvalue $P = P_r + iP_i$ is found by solving the eigenvalue problem numerically. The number of modes l is increased until convergence to a prescribed accuracy is achieved. For example, if we take $l = 0$ (the smallest possible value of l), we obtain

$$\begin{vmatrix} p + \alpha^4 K^4 C - i\alpha(V_0 + W) & \alpha^2 K^2 C \\ i\alpha K + \tfrac{3}{2}\alpha^4 K^4 C & p + 2\alpha^2 K^2 C - i\alpha(V_0 + W) \end{vmatrix} = 0, \tag{5.5}$$

where $C = C_0(1-\epsilon)$. This equation does not capture the interaction of the disturbance with the primary saturated solution; only the basic uniform flow is involved. However, this interaction will appear starting with $l = 1$, in the homogeneous equations for $\{B_{-1}, C_{-1}, B_0, C_0, B_1, C_1\}$. For example, the top row in the coefficient matrix of the homogeneous system, keeping only the leading-order terms, $O(1)$, and the first correction terms, $O(\epsilon^{1/2})$, is as follows:

$$\left.\begin{array}{lll} p + \alpha^4 K_-^4 C_0 - i\alpha K_- V_0, & \alpha^2 K_-^2 C_0, & \\ \left(i\alpha + 3C\alpha^4(K^3 - 1)\right) K_- A_{1(\alpha)}^* - 2C\alpha^2 K_- B_{1(\alpha)}^*, & 2C\alpha^2 K K_- A_{1(\alpha)}^*, & \\ \left(i\alpha + 3C\alpha^4(K_+^3 - 2^3)\right) K_- A_{2(\alpha)}^* - 4C\alpha^2 K_- B_{2(\alpha)}^*, & 2C\alpha^2 K_+ K_- A_{2(\alpha)}^*, & \end{array}\right\} \tag{5.6}$$

where $K_- = K - 1$ and $K_+ = K + 1$. We do not show the remaining five rows which are obtained similarly. In fact we took into account the higher-order, $O(\epsilon)$, terms including the last term of (5.1), in the saturated primary-instability state.

We are interested in the value of K and the corresponding eigenvalue whose real part is the largest. This maximum real part, $M = max\, P_r$, which is the growth rate of the instability, is shown as a function of the primary wavenumber α in figure 18 for three different values of ϵ. The corresponding value of the Bloch's wavenumber K at which the maximum growth rate occurs is shown in figure 19. The fact that the values of M are everywhere positive shows that the steady periodic states are always unstable to disturbances containing longer waves. We have observed that the curve in figure 19 with $\epsilon = 10^{-8}$ is practically indistinguishable from the one (not shown here) of the maximum growth rate vs the marginal wavenumber α of the *primary* instability. This indicates that for very small ϵ, the primary wavy flow is negligible and the secondary instability is caused by interaction directly with the basic, flat-film, uniform flow. For larger ϵ and sufficiently long waves, as the horizontal parts in figure 19 show, the primary modes with half the wavenumber are responsible for the secondary instability, which thus has a subharmonic character.

We have also (numerically) followed the evolution of disturbances (of the same travelling-wave equilibria) using the full PDEs (2.17) and (2.18). If the computational domain is long enough to allow for sufficiently long-wave disturbances, the amplitudes of η and g grow due to the secondary instability and reach values of order 1. The weakly nonlinear equations are expected be good for small amplitudes. However, as

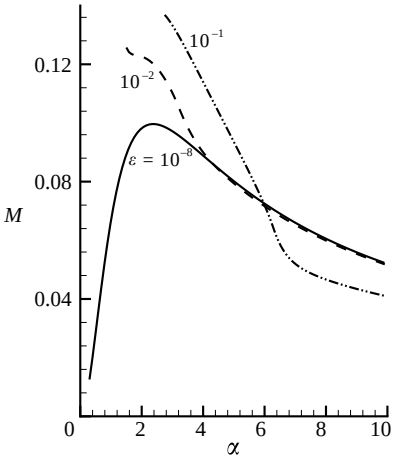

FIGURE 18. Maximum growth rate of the secondary instability M as a function of the primary wavenumber α for three values of ϵ.

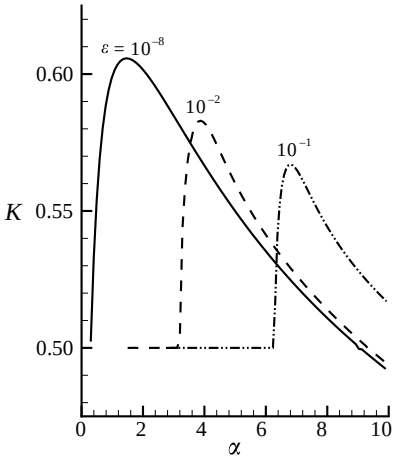

FIGURE 19. Secondary wavenumber K of the fastest growing mode vs the primary wavenumber α.

figure 20 shows, when C_0 is small, the WNPDEs give a good description of saturation even though the saturation amplitude of the surfactant concentration is large. The profiles of saturated waves shown in figure 21 are large-amplitude and non-sinusoidal. At a larger value of C_0, figure 22 shows that the strongly nonlinear evolution leads to saturation at large amplitudes. The WNPDE evolution (not shown) turns out to be very close to the strongly nonlinear one up to the point marked on the curve in figure 22; however, the weakly nonlinear amplitudes blow up beyond that point. Figure 23 testifies that as C_0 increases, the profiles become progressively more non-sinusoidal. In all cases, the initial exponential growth of small disturbances confirms the results of the linear theory of the secondary instability.

6. Discussion and conclusions

For the semi-infinite Couette-film flow with an insoluble surfactant at the interface, we have concentrated on the parametric regimes in which the marginal wavelength

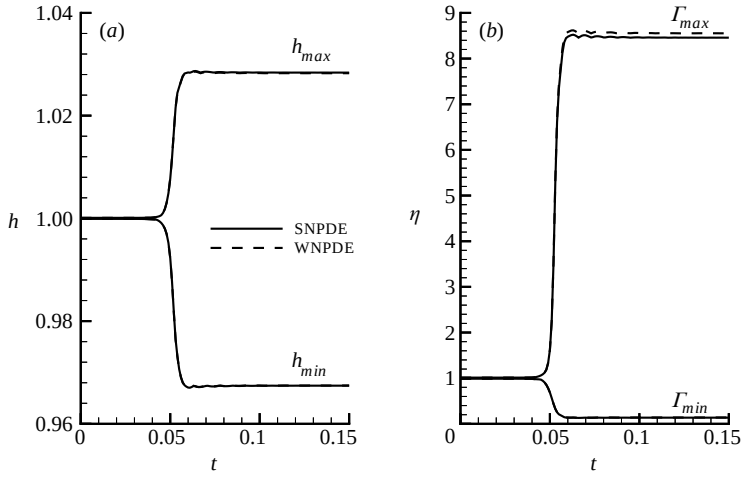

FIGURE 20. Typical saturation evolutions of the secondary instability for (*a*) the film thickness and (*b*) the surfactant concentration ($C_0 = 10^{-4}$, $\epsilon = 10^{-4}$ and the domain length is four times the primary wavelength).

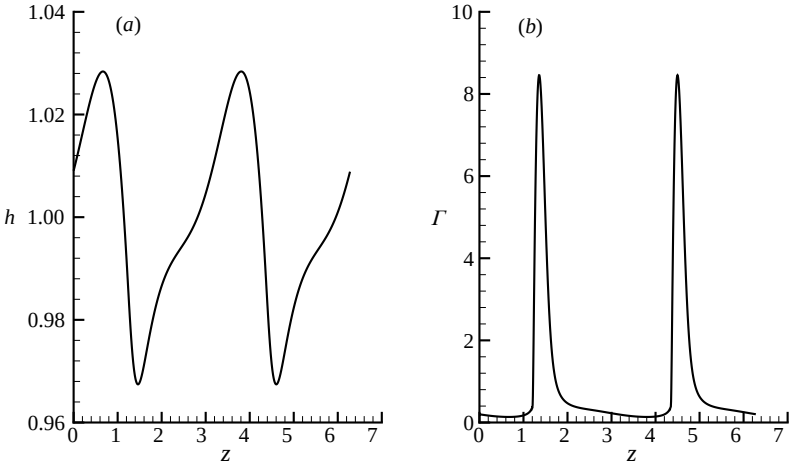

FIGURE 21. Saturated profiles of (*a*) the film thickness and (*b*) the surfactant concentration (here, $C_0 = 10^{-4}$, $\epsilon = 10^{-4}$ and the domain length is four times the primary wavelength).

of the interfacial-surfactant instability is much larger than the basic film thickness and the lubrication approximation is valid in the film (see Frenkel & Halpern 2006). We have obtained the WNPDEs appropriate for disturbances whose spatial period is close to the marginal wavelength.

The latter are different from both the general SNPDEs and the WNPDEs appropriate for disturbances of longer wavelengths. They have some features in common: each of the three systems consists of two PDEs, couples the film thickness and surfactant concentration and is rescaled to a canonical form which is controlled by a single parameter, the 'shear-Marangoni number' C. For the values of C below some separating value C_s, our strongly nonlinear simulations uncovered saturation to small-amplitude travelling waves. Such saturation should be amenable to an approximate description with the WNPDEs, and our simulations of the latter confirm

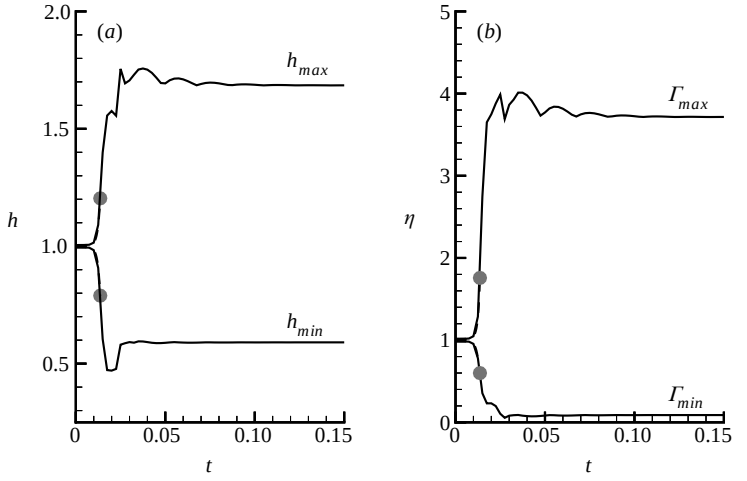

FIGURE 22. SNPDE evolution similar to the one in figure 20 but for $C_0 = 10^{-1}$. The WNPDE follows the curve very closely up to the points on the curves marked by circles; for larger times the amplitudes of the WNPDE blow up in a very short time.

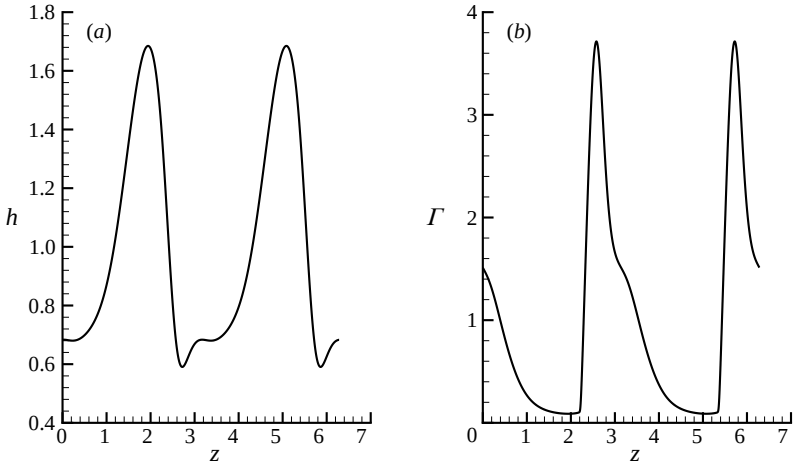

FIGURE 23. Saturated profiles of (*a*) the film thickness profiles and (*b*) the surfactant concentration ($C_0 = 10^{-1}$, $\epsilon = 10^{-4}$ and the domain length is four times the primary wavelength).

that such is the case. Moreover, we have obtained a Stuart–Landau ODE for an amplitude describing the (unstable) fundamental mode, by taking into account the (two) half-wavelength linearly damped harmonics which are nonlinearly excited by the fundamental mode. We have demonstrated that this ODE is capable of approximating the process of saturation, and that its error dies out as expected as the conditions approach the marginal case.

For shear-Marangoni numbers larger than the separating value C_s, the Hopf bifurcation to the travelling waves in the Stuart–Landau equation is subcritical, in contrast to the supercritical bifurcation for $C < C_s$. The strongly nonlinear saturation is still possible, but cannot be expected to be described all the way to the very end by either the WNPDEs or the Stuart–Landau ODE. In fact, in a case study (see figure 8)

in which the SNPDEs show saturation, solutions of both the WNPDE system and of the Stuart–Landau equation blow up at a finite time (remaining close to each other up to the instant when the simulation run had to be stopped).

We have studied the change of the travelling-wave equilibria as the wavenumber is decreased out of the near-marginal domain, by continuation of the solutions of the dynamical-system generated by the SNPDEs, with the spatial coordinate being the independent variable of the dynamical ODEs (and with the time dependence being eliminated by changing to the reference frame affixed to the wave). The results (obtained with the continuation and bifurcation software for ODEs, AUTO-07P (Doedel *et al.* 2006) and presented, for the closed flow condition, in figures 12–14) confirm that there is a value C_s of C, confined to the interval $0.2 < C_s < 0.4$, such that the bifurcation from the basic uniform flow is supercritical for $C < C_s$ but becomes subcritical for $C > C_s$ (more precisely, $C_s \approx 0.29$). For the subcritical continuation curves, there is a region of wavenumbers (delimited below by the marginal one, and above by the value corresponding to a saddle-node bifurcation) for which there are two amplitude values for each wavenumber. As is usual in such cases, only the equilibrium with the larger amplitude is stable (as a periodic orbit of the dynamical system) and the other one is unstable. The spatial profiles of the film thickness and surfactant concentration have some interesting features. For the open flow condition, the results (presented in figures 15–17) indicate, in particular, that the value C_s separating supercritical and subcritical regimes is larger than the one for the closed flow condition; for the open flow case, $0.4 < C_s < 0.6$. For large C, the film thickness tends to zero at a point and the surfactant concentration develops a steep front.

We have considered the stability of the travelling-wave solutions when the disturbances of larger wavelengths than that of the primary wave are admitted. To this end, we linearized the PDEs about the steady space-periodic primary equilibria, and used the Bloch ('Floquet') disturbance modes. All the small-amplitude travelling waves turned out to be unstable to sufficiently long-wave disturbances. This theoretical result was borne out with numerical simulation of both the SNPDEs and WNPDEs, starting with the travelling-wave solutions of a near-marginal wavelength which were slightly disturbed by long-wave additives. The disturbances grew until eventually saturation happened in the strongly nonlinear evolution, but with at least one of the saturated amplitudes being not small. For smaller values of C, where characteristically the saturated amplitudes of film thickness are small but those of surfactant concentration are large, the WNPDEs, somewhat surprisingly, are still good for all time. However, for larger values of C, the weakly nonlinear solutions follow the underlying strongly nonlinear evolution only as long as the amplitudes are small, but afterwards they part from the saturating strongly nonlinear solutions and blow up at finite time (see figure 22).

In view of the fact that the secondary instability is unavoidable, the existence of the small-amplitude travelling-wave solutions *is* compatible with the observation (see Frenkel & Halpern 2006) that for at least one of the two unknowns (the film thickness and the surfactant concentration) the disturbance becomes large-amplitude in the course of evolution. For the near-criticality conditions, this suggests that the amplitudes of saturated disturbances may not decrease to zero as the control parameter approaches its critical value (and the corresponding marginal wavenumber approaches zero, see figure 3*a*). This is in contrast to the case of instabilities with a non-zero wavenumber at criticality (where the saturation is described by the Stuart–Landau equation or its PDE counterpart, the Ginzburg–Landau equation). More remarkably, the previously known cases of instabilities with zero wavenumber at

criticality with the evolution of disturbances being governed by equations of the Kuramoto–Sivashinsky type featured small-amplitude saturation (see, e.g., Babchin *et al.* 1983 for the Rayleigh–Taylor instability, Hooper & Grimshaw 1985 for the Yih instability, Frenkel *et al.* 1987 for the instability of core-annular flows, and Sivashinsky & Michelson 1980 for the instability of falling films), perhaps suggesting that the near-critical small-amplitude saturation is a general property of such instabilities as well. However, the interfacial-surfactant instability appears to provide a counterexample. The key to the special character of this instability might be the fact that the corresponding dispersion curves are very wide, as in figure 3(*b*). Indeed, in the Ginzburg–Landau ('non-zero criticality') case, the weakly unstable modes comprise a narrow band and interact only with finitely-damped modes far outside this unstable band. In the Kuramoto–Sivashinsky zero-criticality case, the modes with the near-maximum growth rate comprise a somewhat similar, comparatively narrow band of wavenumbers around α_{max}, with the limiting value $\alpha_0/\alpha_{max} = \sqrt{2} < 2$, so the first overtones are already finitely damped. In contrast, as figure 3(*c*) testifies, $\alpha_0/\alpha_{max} \to \infty$ in our case. This allows the slightly damped modes, which are just to the right of α_0, to be excited to a level comparable to the unstable modes. If this is the case, the energy balance may be compatible with the amplitudes of both the weakly unstable and the weakly damped modes remaining finite as the control parameter approaches its criticality value.

Speaking of the weakly-nonlinear equations which are appropriate near criticality, it is clear that they can describe all pertinent small disturbances. In contrast, the Stuart–Landau equation appropriate near *marginality* (see also, e.g., Lin 1974; Cheng & Chang 1990; Chang *et al.* 1993; Scheid *et al.* 2005) is restricted to (small-amplitude) disturbances whose spatial periods are close to the marginal wavelength. Therefore, the equilibrium solutions of this equation are, typically, unstable – e.g. to disturbances with larger spatial periods. Nevertheless, since the unstable 'fixed points' (in *infinite-dimensional* phase space, in this case) imply that the dynamics in their vicinities is slow, the travelling-waves equilibria may be approximately realized as quasi-stationary states, that is wave patterns which persist for a sufficiently long time to be observable in experiments (see Pugh & Saffman 1998).

Appendix A. Equations of the full Navier–Stokes problem

Here, we include, as a reference point, the complete formulation of the problem (which, by using pertinent approximations, becomes significantly simplified in § 2).

The Navier–Stokes and incompressibility equations governing the fluid motion in the two layers are (with $j = 1$ for the lower layer and $j = 2$ for the upper one)

$$\rho\left(\frac{\partial \boldsymbol{v}_j^*}{\partial t^*} + \boldsymbol{v}_j^*\cdot\nabla^*\boldsymbol{v}_j^*\right) = -\nabla^* p_j^* + \mu_j\nabla^{*2}\boldsymbol{v}_j^*, \quad \nabla^*\cdot\boldsymbol{v}_j^* = 0, \tag{A 1}$$

where $\nabla^* = (\partial/\partial x^*, \partial/\partial y^*)$, ρ is the density (of both fluids), $\boldsymbol{v}_j^* = (u_j^*, v_j^*)$ is the fluid velocity with the horizontal component u_j^* and vertical component v_j^*, and p_j^* is the pressure.

The boundary conditions at the plates are $u_1^* = 0$, $v_1^* = 0$ at $y^* = 0$ and $u_2^* = U_2$, $v_2^* = 0$ at $y^* = d_1 + d_2$, where U_2 is the velocity of the upper plate. The interfacial boundary conditions are: the velocity continuity at the interface, $[\boldsymbol{v}^*]_1^2 = 0$, where $[A]_1^2 = A_2 - A_1$ denotes the jump in A across the interface, i.e. at $y^* = h^*(x^*, t^*)$; the balance of the tangential and normal stresses taking into account the jump in the tangential stress (due to the variability of surface tension) as well as the capillary

jump in the normal stress, at $y^* = h^*(x^*, t^*)$, are

$$\frac{1}{1+h_{x^*}^{*2}}[(1-h_{x^*}^{*2})\mu(u_{y^*}^* + v_{x^*}^*) + 2h_{x^*}^{*2}\mu(v_{y^*}^* - u_{x^*}^*)]_1^2 = -\frac{\sigma_{x^*}^*}{(1+h_{x^*}^{*2})^{1/2}},$$
$$[(1+h_{x^*}^{*2})p^* - 2\mu(h_{x^*}^{*2}u_{x^*}^* - h_{x^*}^*(u_{y^*}^* + v_{x^*}^*) + v_{y^*}^*)]_1^2 = \frac{h_{x^*x^*}^*}{(1+h_{x^*}^{*2})^{1/2}}\sigma^*,$$

where σ^* is the surface tension (the subscripts x^*, y^*, t^* denote the derivative with respect to that variable); the kinematic boundary condition (the conservation of mass condition)

$$\frac{\partial h^*}{\partial t^*} + \frac{\partial}{\partial x^*}\int_0^{h^*(x^*,t^*)} u^*\,\mathrm{d}y^* = 0; \tag{A 2}$$

and the equation for the surface concentration of the insoluble surfactant, $\Gamma^*(x^*, t^*)$, (see a simple derivation in Halpern & Frenkel 2003):

$$\frac{\partial(H\Gamma^*)}{\partial t^*} + \frac{\partial}{\partial x^*}\left(H\Gamma^* u^*\right) = D_s\frac{\partial}{\partial x^*}\left(\frac{1}{H}\frac{\partial\Gamma^*}{\partial x^*}\right), \tag{A 3}$$

where $H = \sqrt{1+h_x^{*2}}$, and D_s is the surface molecular diffusivity of surfactant; D_s is usually negligible and is discarded.

Appendix B. Derivation of the Stuart–Landau equation

Here, we derive a Stuart–Landau equation (see (B 18)) for the fundamental amplitude $A_{1(\alpha)}$ of (4.2) and give the expressions of other amplitudes in terms of the fundamental one (see (B 17)).

We substitute the ansatz (4.2) into the weakly nonlinear equations (2.17) and (2.18) augmented with the linear terms containing the speed V_0, the same as in (3.3) and (3.4), and recast into a vector form

$$\frac{\mathrm{d}}{\mathrm{d}t}\begin{bmatrix}\eta\\ g\end{bmatrix} = L_{(\alpha)}\begin{bmatrix}\eta\\ g\end{bmatrix} + \boldsymbol{N}, \tag{B 1}$$

where $\boldsymbol{N}$ stands for the vector of nonlinear terms,

$$\boldsymbol{N} = -\begin{bmatrix}\eta\eta_\xi + 3C(\eta\eta_{\xi\xi\xi})_\xi - 2C(\eta g_\xi)_\xi\\ 3C(\eta\eta_{\xi\xi\xi})_\xi + (\eta g)_\xi - 2C(\eta g_\xi)_\xi + \frac{3}{2}C(\eta_{\xi\xi\xi}g)_\xi - 2C(gg_\xi)_\xi\end{bmatrix}. \tag{B 2}$$

This yields the equation

$$\sum_{k,n}\left(\frac{\mathrm{d}}{\mathrm{d}t}A_{k(n\alpha)}\right)\begin{bmatrix}1\\ g_{k(n\alpha)}\end{bmatrix}\mathrm{e}^{\mathrm{i}n\alpha\xi} = \sum_{k,n}\lambda_{k(n\alpha)}\begin{bmatrix}1\\ g_{k(n\alpha)}\end{bmatrix}A_{k(n\alpha)}\mathrm{e}^{\mathrm{i}n\alpha\xi} + \text{c.c.} + \boldsymbol{N}, \tag{B 3}$$

where both k and n run over the values $\{1, 2\}$. Truncating at the leading order, we have

$$\boldsymbol{N} = -\mathrm{i}\alpha\mathrm{e}^{\mathrm{i}\alpha\xi}A_{1(\alpha)}^*\left(A_{1(2\alpha)}\boldsymbol{N}_{1(\alpha)} + A_{2(2\alpha)}\boldsymbol{N}_{2(\alpha)}\right) - 2\mathrm{i}\alpha\mathrm{e}^{\mathrm{i}2\alpha\xi}A_{1(\alpha)}^2\boldsymbol{M} + \text{c.c.}, \tag{B 4}$$

where

$$\boldsymbol{N}_{k(\alpha)} = \begin{bmatrix}1 - \mathrm{i}\alpha C(21\alpha^2 + 4g_{k(2\alpha)} - 2g_{1(\alpha)}^*)\\ g_{k(2\alpha)} + g_{1(\alpha)}^* - \mathrm{i}\alpha C\left(21\alpha^2 + \left(4 - \frac{3}{2}\alpha^2\right)g_{k(2\alpha)} - 2\left(1 - 6\alpha^2 - g_{k(2\alpha)}\right)g_{1(\alpha)}^*\right)\end{bmatrix} \tag{B 5}$$

(for $k = 1, 2$) and

$$\boldsymbol{M} = \begin{bmatrix} \frac{1}{2} - \mathrm{i}\alpha C\left(3\alpha^2 + 2g_{1(\alpha)}\right) \\ g_{1(\alpha)} - \mathrm{i}\alpha C\left(3\alpha^2 + \left(2 + \frac{3}{2}\alpha^2\right) g_{1(\alpha)} + 2g_{1(\alpha)}^2\right) \end{bmatrix}. \tag{B 6}$$

The vectors $\boldsymbol{N}_{k(\alpha)}$ and $\boldsymbol{M}$ can be expanded into standard basis as follows:

$$\boldsymbol{N}_{k(\alpha)} = \begin{bmatrix} N_{1(k(\alpha))} \\ N_{2(k(\alpha))} \end{bmatrix} = a_k \begin{bmatrix} 1 \\ g_{1(\alpha)} \end{bmatrix} + b_k \begin{bmatrix} 1 \\ g_{2(\alpha)} \end{bmatrix}, \tag{B 7}$$

where

$$a_k = \frac{N_{2(k(\alpha))} - N_{1(k(\alpha))} g_{2(\alpha)}}{g_{1(\alpha)} - g_{2(\alpha)}}, \quad b_k = \frac{N_{1(k(\alpha))} g_{1(\alpha)} - N_{2(k(\alpha))}}{g_{1(\alpha)} - g_{2(\alpha)}}, \tag{B 8}$$

and

$$\boldsymbol{M} = \begin{bmatrix} M_1 \\ M_2 \end{bmatrix} = e \begin{bmatrix} 1 \\ g_{1(2\alpha)} \end{bmatrix} + f \begin{bmatrix} 1 \\ g_{2(2\alpha)} \end{bmatrix}, \tag{B 9}$$

where

$$e = \frac{M_2 - M_1 g_{2(2\alpha)}}{g_{1(2\alpha)} - g_{2(2\alpha)}}, \; f = \frac{M_1 g_{1(2\alpha)} - M_2}{g_{1(2\alpha)} - g_{2(2\alpha)}}. \tag{B 10}$$

So, $\boldsymbol{N}$ is expressed as a linear combination of the standard basis vectors (those appearing in the linear terms):

$$\begin{aligned} \boldsymbol{N} = &- \mathrm{i}\alpha \mathrm{e}^{\mathrm{i}\alpha\xi} A_{1(\alpha)}^{*} \left(a_1 A_{1(2\alpha)} + a_2 A_{2(2\alpha)}\right) \begin{bmatrix} 1 \\ g_{1(1\alpha)} \end{bmatrix} \\ &- 2\mathrm{i}\alpha \mathrm{e}^{\mathrm{i}2\alpha\xi} A_{1(\alpha)}^2 \left(e \begin{bmatrix} 1 \\ g_{1(2\alpha)} \end{bmatrix} + f \begin{bmatrix} 1 \\ g_{2(2\alpha)} \end{bmatrix} \right). \end{aligned} \tag{B 11}$$

Thus, by substituting $\boldsymbol{N}$ into (B 3) and equating the coefficients of the (linear independent) basis vectors we obtain the following amplitude equations for the unstable fundamental mode and the overtones:

$$\frac{\mathrm{d}A_{1(\alpha)}}{\mathrm{d}t} = \lambda_{1(\alpha)} A_{1(\alpha)} - \mathrm{i}\alpha A_{1(\alpha)}^{*} \left(a_1 A_{1(2\alpha)} + a_2 A_{2(2\alpha)}\right), \tag{B 12}$$

$$\frac{\mathrm{d}A_{1(2\alpha)}}{\mathrm{d}t} = \lambda_{1(2\alpha)} A_{1(2\alpha)} - 2\mathrm{i}\alpha e A_{1(\alpha)}^2, \tag{B 13}$$

$$\frac{\mathrm{d}A_{2(2\alpha)}}{\mathrm{d}t} = \lambda_{2(2\alpha)} A_{2(2\alpha)} - 2\mathrm{i}\alpha f A_{1(\alpha)}^2. \tag{B 14}$$

It is important to note that, as is seen from (3.13), $\lambda_{1(\alpha)}$ is small, but $\gamma_{k(2\alpha)}$ is not small (and $\gamma_{2(\alpha)}$ is not small as well):

$$\lambda_{1(\alpha)} = O(\epsilon), \tag{B 15}$$

$$\lambda_{k(2\alpha)} = O(1), \; \gamma_2(\alpha) = O(1). \tag{B 16}$$

The overtones may feature initial fast-decaying transients which die out quickly since (the negative) $\gamma_k(2\alpha)$ are $O(1)$. Except for the short time during which these transients decay, the time derivatives in the left-hand side of (B 13) and (B 14) can be neglected (indeed, it will be seen that $d/dt = O(\epsilon)$ so that the left-hand sides are $O(\epsilon^2)$ whereas the right-hand sides are $O(\epsilon)$), and so the overtones are slaved to the fundamental mode:

$$A_{1(2\alpha)} = \frac{2\mathrm{i}\alpha e}{\lambda_{1(2\alpha)}} A_{1(\alpha)}^2, \; A_{2(2\alpha)} = \frac{2\mathrm{i}\alpha f}{\lambda_{2(2\alpha)}} A_{1(\alpha)}^2. \tag{B 17}$$

(This corresponds to the equations of the centre manifold in the leading order, e.g., similar to § 8.2 of Glendinning 1994.) Substituting these two expressions into (B 12) yields the Stuart–Landau equation for the fundamental amplitude $A_{1(\alpha)}$ (see, e.g., (49.10) of Drazin & Reid 1981):

$$\frac{\mathrm{d}A_{1(\alpha)}}{\mathrm{d}t} = sA_{1(\alpha)} - \tfrac{1}{2}\ell|A_{1(\alpha)}|^2 A_{1(\alpha)}, \tag{B 18}$$

where

$$s = \lambda_{1(\alpha)} \tag{B 19}$$

and the Landau constant ℓ is given by

$$\ell = -4\alpha^2 \left(\frac{a_1 e}{\lambda_{1(2\alpha)}} + \frac{a_2 f}{\lambda_{2(2\alpha)}} \right). \tag{B 20}$$

Since $s = O(\epsilon)$ and $\ell = O(1)$, the two terms in the right-hand side are of the same order, $O(\epsilon^{3/2})$, when $A_{1(\alpha)} = O(\epsilon^{1/2})$. It follows that, for the left-hand side to be of the same order as the right-hand side, it must be that $\mathrm{d}/\mathrm{d}t = O(\epsilon)$. (This is consistent with the slow evolution on the centre manifold. In contrast, if the system is initially off the centre manifold, it approaches the latter in fast time, as described by (B 13), (B 14) and (B 16).)

REFERENCES

Babchin, A. J., Frenkel, A. L., Levich, B. G. & Sivashinsky, G. I. 1983 Flow-induced nonlinear effects in thin liquid film stability. *Ann. NY Acad. Sci.* **404**, 426–428.

Barthelet, P., Charru, F. & Fabre, J. 1995 Experimental study of interfacial long waves in a 2-layer shear-flow. *J. Fluid Mech.* **303**, 23–53.

Blennerhassett, P. J. 1980 On the generation of waves by wind. *Proc. R. Soc. Lond.* A **298**, 451–494.

Blyth, M. G. & Pozrikidis, C. 2004*a* Effect of inertia on the Marangoni instability of two-layer channel flow, Part II: normal-mode analysis. *J. Engng Maths* **50**, 329–341.

Blyth, M. G. & Pozrikidis, C. 2004*b* Effect of surfactants on the stability of two-layer channel flow. *J. Fluid Mech.* **505**, 59–86.

Chang, H. C., Demekhin, E. A. & Kopelevich, D. I. 1993 Nonlinear evolution of waves on a vertically falling film. *J. Fluid Mech.* **250**, 433–480.

Chen, K. & Joseph, D. D. 1991 Lubricated pipelining: stability of core-annular flow. Part 4. Ginzburg–Landau equations. *J. Fluid Mech.* **227**, 587–615.

Cheng, M. & Chang, H. C. 1990 A generalized side-band stability theory via center manifold projection. *Phys. Fluids* A **2**, 1364–1379.

Doedel, E. J., Champneys, A. R., Fairgrieve, T., Kuznetsov, Y., Oldeman, B., Paffenroth, R., Sandstede, B. & Wang, X. 2006 *Auto-07P: Continuation and Bifurcation Software for Ordinary Differential Equations*.

Dong, L. & Johnson, D. 2005 Experimental and theoretical study of the interfacial instability between two shear fluids in a channel Couette flow. *Int. J. Heat Fluid Flow* **26**, 133–140.

Drazin, P. G. & Reid, W. H. 1981 *Hydrodynamic Stability*. Cambridge University Press.

Frenkel, A. L. 1991 Stability of an oscillating Kolmogorov flow. *Phys. Fluids* A **3**, 1718–1729.

Frenkel, A. L., Babchin, A. J., Levich, B. G., Shlang, T. & Sivashinsky, G. I. 1987 Annular flow can keep unstable flow from breakup: nonlinear saturation of capillary instability. *J. Colloid Interface Sci.* **115**, 225–233.

Frenkel, A. L. & Halpern, D. 2002 Stokes-flow instability due to interfacial surfactant. *Phys. Fluids* **14**, L45–L48.

Frenkel, A. L. & Halpern, D. 2005 Effect of inertia on the insoluble-surfactant instability of a shear flow. *Phys. Rev.* E **71**, 016302.

Frenkel, A. L. & Halpern, D. 2006 Strongly nonlinear nature of interfacial-surfactant instability of Couette flow. *Intl J. Pure Appl. Maths* **29**, 205–224. [arXiv:nlin/0601025]

Frenkel, A. L. & Indireshkumar, K. 1996 Derivation and simulations of evolution equations of wavy film flows. In *Math Modeling and Simulation in Hydrodynamic Stability* (ed. D. N. Riahi), pp. 35–81. World Scientific.

Gao, G. P. & Lu, X. Y. 2006 Effect of surfactants on the long-wave stability of oscillatory film flow. *J. Fluid Mech.* **562**, 345–354.

Gjevik, B. 1970 Occurrrence of finite-amplitude surface waves on falling liquid films. *Phys. Fluids* **13**, 1918–1925.

Glendinning, P. 1994 *Stability, Instability, and Chaos: An Introduction to the Theory of Nonlinear Differential Equations*. Cambridge University Press.

Golubitsky, M., Stewart, I. & Schaeffer, D. G. 1988 *Singularities and Groups in Bifurcation Theory: Volume 2*. Springer.

Halpern, D. & Frenkel, A. L. 2003 Destabilization of a creeping flow by interfacial surfactant: Linear theory extended to all wavenumbers. *J. Fluid Mech.* **485**, 191–220.

Halpern, D., Naire, S., Jensen, O. E. & Gaver, D. P. 2005 Unsteady bubble propagation in a flexible channel: predictions of a viscous stick-slip instability. *J. Fluid Mech.* **528**, 53–86.

Herbert, T. 1988 Secondary instability of boundary-layers. *Annu. Rev. Fluid Mech.* **20**, 487–526.

Hooper, A. P. 1985 Long-wave instability at the interface between two viscous fluids: Thin layer effects. *Phys. Fluids* **28**, 1613–1618.

Hooper, A. P. & Grimshaw, R. 1985 Nonlinear instability at the interface between two viscous fluids. *Phys. Fluids* **28**, 37–45.

Indireshkumar, K. & Frenkel, A. L. 1996 Spatiotemporal patterns in a 3-D film flow. In *Advances in Multi-Fluid Flows (Proc. AMS–IMS–SIAM Summer Research Conference, Seattle, 1995)* (ed. Y. Renardy), pp. 288–309. Society for Industrial and Applied Mathematics, Philadelphia.

Jensen, O. E. & Grotberg, J. B. 1992 Insoluble surfactant spreading on a thin viscous film: shock evolution and film rupture. *J. Fluid Mech.* **240**, 259–288.

Joseph, D. D. & Renardy, Y. 1993 *Fundamentals of Two-Fluid Dynamics, vol I: Mathematical Theory and Applications*. Springer.

Kelly, R. E. 1967 On stability of an inviscid shear layer which is periodic in space and time. *J. Fluid Mech.* **27**, 657–689.

Leshansky, A. M. & Rubinstein, B. Y. 2005 Nonlinear rupture of thin liquid films on solid surfaces. *Phys. Rev.* E **71**, 040601.

Levy, R. & Shearer, M. 2006 The motion of a thin liquid film driven by surfactant and gravity. *SIAM J. Appl. Maths* **66**, 1588–1609.

Lin, S. P. 1974 Finite-amplitude side-band stability of a viscous film. *J. Fluid Mech.* **63**, 417–429.

Oron, A., Davis, S. H. & Bankoff, S. G. 1997 Long–scale evolution of thin liquid films. *Rev. Mode. Phys.* **69**, 931–980.

Pugh, J. D. & Saffman, P. G. 1998 Two-dimensional superharmonic stability of finite-amplitude waves in plane Poiseuille flow. *J. Fluid Mech.* **194**, 295–307.

Renardy, Y. 1989 Weakly nonlinear behavior of periodic disturbances in two-layer Couette–Poiseuille flow. *Phys. Fluids* A **1**, 1666–1676.

Scheid, B., Ruyer-Quil, C., Thiele, U., Kabov, O. A., Legros, J. C. & Colinet, P. 2005 Validity of the Benney equation including the Marangoni effect for closed and open flows. *J. Fluid Mech.* **527**, 303–335.

Schwartz, L. W., Weidner, D. E. & Eley, R. R. 1995 An analysis of the effect of surfactant on the leveling behavior of a thin liquid coating layer. *Langmuir* **11**, 3690–3693.

Shlang, T., Sivashinsky, G.I., Babchin, A. J. & Frenkel, A. L. 1985 Irregular wavy flow due to viscous stratification. *J. Phys. (Paris)* **46**, 863–866.

Sivashinsky, G. I. & Michelson, D. M. 1980 On irregular wavy flow of a liquid film down a vertical plane. *Prog. Theor. Phys.* **63**, 2112–2114.

Stuart, J. T. 1960 On the nonlinear mechanics of wave disturbances in stable and unstable parallel flows. Part 1. The basic behaviour in plane Poiseuille flow. *J. Fluid Mech.* **9**, 353–370.

Watson, J. 1960 On the nonlinear mechanics of wave disturbances in stable and unstable parallel flows. Part 2. The development of a solution for plane Poiseuille flow and for plane Couette flow. *J. Fluid Mech.* **9**, 371–389.

Wei, H. H. 2005*a* Effect of surfactant on the long-wave instability of a shear-imposed liquid flow down an inclined plane. *Phys. Fluids* **17**, 012103.

Wei, H. H. 2005*b* Marangoni destabilization on a core-annular film flow due to the presence of surfactant. *Phys. Fluids* **17**, 027101.

Wei, H. H. 2005*c* On the flow-induced Marangoni instability due to the presence of surfactant. *J. Fluid Mech.* **544**, 173–200.

Wei, H. H. 2007 Role of base flows on surfactant-driven interfacial instabilities. *Phys. Rev.* E **75**, 036306.

Wei, H. H. & Rumschitzki, D. S. 2005 The effects of insoluble surfactants on the linear stability of a core-annular flow. *J. Fluid Mech.* **541**, 115–142.

Yih, C. S. 1967 Instability due to viscosity stratification. *J. Fluid Mech.* **27**, 337–352.